PREDICTION OF nsSNPs OF LXR - ALPHA GENE AND VALIDATION OF THEIR ROLE IN VITILIGO SUSEPTIBILITY

ENROLLMENT NO. - 142552

STUDENT NAME - GURJINDER KAUR

SUPERVISOR NAME - Dr. HARISH CHANGOTRA

MAY - 2016

Submitted in partial fulfillment of the requirement for the award of the Degree of

Master of Technology

in

Biotechnology

DEPARTMENT OF BIOTECHNOLOGY AND BIOINFORMATICS

JAYPEE UNIVERSITY OF INFORMATION AND TECHNOLOGY

WAKNAGHAT, SOLAN – 173234, HIMACHAL PRADESH

TABLE OF CONTENTS

CERTIFICATE

This is to certify that the work titled "**Prediction of nsSNPs of LXR alpha gene and validation of their role in Vitiligo susceptibility**", submitted by "**Gurjinder Kaur**" in partial fulfillment for the award of degree of **Master of Technology in Biotechnology** of Jaypee University of Information Technology, Waknaghat has been carried out under my supervision. This work has not been submitted partially or wholly to any other University or Institute for the award of this or any other degree or diploma.

Signature of Supervisor:

Harish Changotra, Ph.D.

(Associate Professor)
Department of Biotechnology and Bioinformatics
Jaypee University of Information Technology
Solan, Himachal Pradesh 173 234, INDIA

ACKNOWLEDGEMENT

Gratitude, they say, cannot be seen, it can only be felt and feelings of heart are hard to describe. Here I fail to describe in words my heart felt gratitude to my revered and honourable teachers and everlasting encouragement from all dear and near ones, in successful completion of well cherished task in the scientific methodology.

Research is a high concept. it brings to test our patience, vigour and dedication. Every result arrived is a beginning for a higher achievement. My project is the same, it is just a drop in an ocean. It needs the help of friends and guidance of experts in the field, to achieve something new.

First and foremost, being a pupil in Jaypee University of Information Technology (JUIT), I found my pen too incompetent to express my thanks to my guide Dr. Harish Changotra, Associate Professor under whose kind and worthy guidance, and supervision, I have the opportunity to carry out this work. It is only due to his timely advice, thoughtful comments, constructive criticism, and continuous vigil over the progress of my work.

I, greatly, acknowledge **Dr. R.S. Chauhan,** Head of Department for the valuable assistance.

I express my sincere thanks to scholars, Mr. Rohit Randhawa, Mr. Sanjay Singh, Mrs.Ambika Sharma and Ms. Avni Vij for their constant support, valuable suggestion, encouragement and excellent cooperation.

Last but not the least, I whole heartedly thank my parents and my friends, Poonam, Ajay and Nitya who were always there through my thick and thin.

Gurjinder Kaur

Date:

Place: Waknaghat

SUMMARY

Vitiligo is a relatively common, acquired pigmentary disorder characterized by areas of depigmented skin resulting from loss of epidermal melanocytes. In India and perhaps elsewhere also men, women and children with vitiligo face severe psychological and social problems. Multiple etiological factors are considered to be involved synergistically with pathogenesis of Vitiligo. This study explained the role of genetic factors, focusing particularly on LXR-alpha gene. Upregulated expression of LXR-alpha in the melanocytes from perilesional skin as compared to normal skin of vitiligo patient speculates its role in vitiligo pathogenesis. Genetic studies so far, has investigated a close association between gene polymorphism and vitiligo risk. Our previous finding of two SNPs of LXR-α gene has showed their association in vitiligo pathogenesis. Hence, to study polymorphism in a larger population, it was required to sort out the possible functional nsSNPs first. For that, dbSNP database along with other computational tools facilitated to carry out the profiling of nsSNPs in LXR-α gene suggesting that I39V (rs11545529), H339Q (rs78765998) and R355Q (rs61731956) variants of LXR-α gene have potential to introduce alterations in the protein stability and may influence the risk of vitiligo.

Two variants, **rs11545529 (+10906 A>G)** and **rs61731956 (+19640 G >A)** out of above three were genotyped further and investigated to find any association with disease susceptibility.

A total of 78 patient blood samples with 120 control samples with no history of Vitiligo were collected along with the written consent form each donor. DNA samples were isolated from the blood samples and genotyped by PCR-RFLP method.

The allelic frequencies of these two SNPs between vitiligo and control were, rs11545529: p=0.5197; rs61731956: p=0.5318, which suggested no association of minor allele of both the SNP with the vitiligo. **+10906** G and **+109640** A alleles were found to have no relation to the risk of vitiligo. (**rs11545529**: odds ratio (OR) =0.8462; 95% confidence interval (CI) =0.5090-1.4068; **rs61731956:** OR= 0.7568; 95% CI =0.31-1.81).

No significant results were found through this study. Probably different experimental procedures would be required to validate the suggested computational analysis of polymorphic variants as shown in this study. Although insignificant with the causal risk of vitiligo, the study could be

utilized further to dig deep into the etiological factors of this disease providing insight into the disease pathogenesis.

Signature of Student:	Signature of Supervisor:
Name:	Name:
Date:	Date:

LIST OF FIGURES

LIST OF TABLES

ABBREVIATION

nsSNPs	Non-Synonymous Single Nucleotide Polymorphisms
LXR-α	Liver – X Receptor alpha
dbSNP	Single Nucleotide Polymorphism Database
PCR	Polymerase Chain Reaction
RFLP	Restriction Fragment Length Polymorphism
ROS	Reactive Oxygen Species
DDG	Double Delta Gibbs Free energy
EtBr	Ethidium Bromide
GV	Generalized Vitiligo
SLE	Systemic Lupus Erythematosus
GWAS	Genome Wide Association Studies
IL	Inter-Leukins
TNF	Tumor Necrosis Factor
RMSD	Root Mean Square Deviation
EDTA	Ethylene Diamine Tetra Acetic acid
˚C	Degrees Celsius
bp	Base Pair
CI	Confidence Interval
DNA	Deoxyribonucleic Acid
dNTP	Deoxyribonuleoside Triphosphate
Sec	seconds
g	Gram
ml	Milli Litres
µl	Micro Litres
rpm	Rotations Per Minute
MMP	Matrix Metalloproteinases
M	Molar
Min	Minutes

Tris	Tris [Aminomethyl hydroxyethane]
TAE	Tris Acetate EDTA buffer
TE Buffer	Tris EDTA buffer
U	Unit
UVR	Ultra-Violet Rays
V	Volts

CHAPTER 1: INTRODUCTION

Vitiligo is an acquired skin disorder characterized by white and depigmented patches enlarging and becoming more numerous with time. It is due to the disappearance of functioning melanocytes and loss of melanin in the epidermis. The condition can be cosmetically disfiguring and the lesional skin is thus more sensitive to sunburns. It affects 0.1-2% of the world's population, irrespective of gender and race. Etiology is unknown and the several pathogenic hypotheses do not account for the entire spectrum of the disease. Although no full therapeutic solution for vitiligo is available, many options may lead to acceptable results in most patients. According to Vitiligo Research Foundation, India has the highest number of patients followed by China and United States. In India and perhaps elsewhere also men, women and children with vitiligo face severe psychological and social problems. Many vitiligo patients feel distressed and stigmatized by their condition, thus it is an important skin disease having major impact on the quality of life of patients suffering from vitiligo.

June 25th is celebrated as World's Vitiligo Day. It is an initiative aimed to build global awareness about vitiligo, a frequent and often disfiguring skin disease that can have a significantly negative social and psychological impact on patients. Researchers from different areas of the world explored intensively the possible shared susceptibility genes involved in vitiligo and other autoimmune diseases and additional genes that may mediate the vitiligo itself.

Several research institutions such as, The University of Massachusetts Medical School Department of Dermatology, Henry Ford Hospital Department of Dermatology, University of Texas Southwestern Department of Dermatology, Postgraduate Institute of Medical Education & Research Department of Dermatology, Venereology & Leprology are actively working to improve the classification, diagnosis, prognosis and treatment of vitiligo. **This project is an approach, small yet significant towards new findings regarding vitiligo pathogenesis. Focusing particularly over the genetics of the disease, we are currently looking into the presence of the non-synonymous single nucleotide polymorphism as well as their association with vitiligo susceptibility.**

Our previous successful finding resulted in achieving association between SNPs and vitiligo susceptibility (Agarwal S. et al 2016) has motivated this study to explore intensively the role of such variants in disease susceptibility.

In skin physiology and pathology, the significance of Liver X Receptor-alpha (LXR- α) gene has evolved rapidly because of its evident high expression in perilesional skin melanocytes. Genetic studies so far, has investigated a close association between gene polymorphism and vitiligo risk.

Hence, to study polymorphism in a larger population, it is required to sort out the possible functional nsSNPs first. For that, dbSNP database along with other computational tools facilitate to carry out the profiling of nsSNPs in LXR-α gene.

LXR are found to be expressed in the skin tissues such as sebaceous glands, hair follicle, epidermal keratinocyte and fibroblast (Billoni, Buan *et al*., 2000; Russell, Harrison et al. 2007). The function and characteristics of LXRs in skin have been recently widely studied but their expression and function in relation to melanocyte have not yet been investigated so much. Recently, Kumar *et.al.(*Kumar, Parsad *et al., 2010)* demonstrated that LXRs are also expressed in melanocytes. They demonstrated that Liver X receptors (LXRs) are upregulated in the melanocytes from perilesional skin as compared to the normal skin of vitiligo patient. Further, they have shown that LXR-α agonist 22(R)-hydroxycholesterol treatment significantly downregulate the cell adhesion molecule, which leads to the detachment of melanocytes from the basement membrane in perilesional vitiligo skin resulting in melanocytorrhagy (Kumar and Parsad 2012). Such studies strongly demonstrate that LXRs appear to have important role in vitiligo pathogenesis and considered as a potential therapeutic target for vitiligo.

Significance of the study

Change in single nucleotide in the DNA sequence may affect how human develops disease, respond to drug etc. Identification of SNP in a gene associated with the vitiligo can act as a susceptibility marker. Associated nsSNP can be used as an informative marker to track the inheritance of disease genes within the families. It can also be used to develop new therapeutic intervention and can be used as a marker for prediction of a treatment outcome in an individual undergoing a vitiligo therapy. Since, LXR-alpha has been associated with the vitiligo and is a promising drug target in skin. Association of any LXRs nsSNP with vitiligo will help us to predict

the treatment outcome where LXRs act as a therapeutic target. **In a nutshell, the main objective of this study is to elucidate any association between nsSNPs (rs11545529 and rs61731956) in LXR-alpha gene and Vitiligo susceptibility with the help of computational tools of analysis and later the experimental procedures to validate the above.**

CHAPTER 2: REVIEW OF LITERATURE

2.1 STRUCTURE AND PHYSIOLOGY OF SKIN

The skin being the largest structure of the human body, is the complex arrangement of structures, with a range of different, yet important functions. It accounts for about 15% of total adult body weight. The skin protects us from microbes and several external elements, helps regulate body temperature, and permits the sensation of touch, heat and cold. It is composed of three layers: the epidermis, the dermis and subcutaneous tissue (Kanitakis 2002). The outermost layer, the epidermis, consists of specific group of cells known as keratinocytes, which function to synthesize keratin, a long threadlike protein which has a protective role. The middle layer dermis consists of fibrillar structural protein which is called collagen. It also contains lymph vessels, hair follicles, nerve endings and glands, provides nutrients and physical support to the epidermis. The deeper subcutaneous tissue (hypodermis) is made of fat and connective tissue. (James *et al.,* 2006)

EPIDERMIS: COMPOSITION AND ITS DEVELOPMENT

The epidermis is a stratified squamous epithelium layer consisting of two major types of cells: keratinocytes and dendritic cells. The epidermis harbors a number of other cell populations such as, melanocytes, Langerhans cells and Merkel cells.

a) Keratinocytes: Accounts for 80% of the cells in the epidermis. Keratinocytes divide mitotically at the stratum basale and one of the daughter cells migrate upwards to the surface of the outermost layer, epidermis. The more they move away from the basale layer, less nutrition they receive and ultimately die (terminal differentiation, keratinocytes converting into corneocytes by the mechanism of apoptosis) (James *et al.,* 2006). In addition, they accumulate more keratin and provide protection against factors such as, UV radiations, heat, chemicals and microorganisms.
b) Melanocytes: Melanocytes are called dendritic, pigment-synthesizing cells of the epidermal layer of the skin, derived from the neural crest (Chu 2008). Melanocytes have long, slender projections containing melanin granules. These projections extend between the keratinocytes and transfer the melanin granules to them. Melanin is produced in

rounded, membrane-bound organelles called melanosomes (Haake & Hollbrook 1999). The synthesis of melanin, a process known as melanogenesis is a receptor-mediated, hormone-stimulated and enzyme catalyzed series of reactions. It is stimulated by increased UV light exposure and results in the increase in the melanosomes transfer to keratinocytes. This response results in the skin's tanning, which increases the cell's ability to absorb light and thus tends to protect the genetic information in the nucleus from the damaging radiations.

Development of melanocytes

The melanocyte lineage is derived from the neural crest, which originates from neural tube. Following its formation, neural crest cells delaminate from the dorsal of the neural tube by a process of epithelial-to-mesenchymal transition. These neural crest cells are highly migratory and go on to form many specialized structures and tissues in the developing embryo by migration, proliferation and differentiation (Mayor and Theveneau 2013). NC-derived cells include neurons and glial cells of the PNS (Peripheral Nervous System), endocrine cells and melanocytes. Schwann cells, which are the glial cells of the peripheral nervous system, can be dedifferentiated *in vitro* to a glia/melanocyte precursor (Dupin *et al*., 2003)

Transcriptional regulation of Melanocyte identity

Recent studies have revealed a central role of *MITF* in the complex network of interacting genes in melanocyte development. The transcription factor microphthalmia-associated transcription factor (MITF) appears to be the master regulator of melanocyte identity and is embedded within a transcriptional network (Fig. 1) that controls and regulates the development of melanocytes.

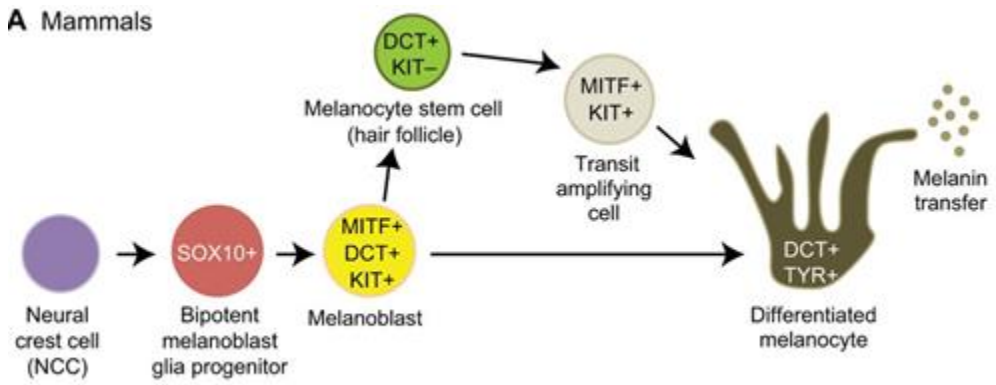

Figure 1: Overview of development of melanocyte (Mort, R.L. *et al*., 2015)

In mammals, melanoblasts are specified from neural crest cells (NCCs) via a SOX10-positive melanoblast/glial bipotent progenitor. SOX10 expression remains switched on in both of these lineages. Melanoblasts under the acquired MITF, DCT and KIT expression colonize into developing embryonic hair follicles, some melanoblasts differentiate into melanocytes and produce the pigment (melanin). A subset of melanoblasts dedifferentiate to form melanocyte stem cells that replenish the differentiated melanocytes through a rapidly proliferating transit-amplifying cell.

2.2 MELANOGENESIS

The skin has epidermal units which are responsible for melanin production and distribution, and it is defined by the process called melanogenesis. These units are composed of a melanocyte surrounded by keratinocytes and is being regulated through hormonal control. Melanin is the primary determinant of skin, hair, and eye color. Melanogenesis occur in the membrane bound organelle named as **melanosomes**. (Simon *et al*., 2009). In the epidermis, each melanocyte interacts through dendrites with 30 to 40 keratinocytes, allowing **transfer of mature melanosomes to the cytoplasm of keratinocytes** positioned strategically over nuclei (Lin, J.Y. *et al*.,2007)

Phenotypic diversity of pigmentation is not due to a variation in melanocyte number, which is relatively constant in different ethnic groups, but to the size and number of melanosomes, the

amount and type of melanin, and melanin transfer and distribution in keratinocytes (Costin GE *et al*., 2007).

There are two types of melanin: **eumelanin** brown-black or dark insoluble polymer - and **pheomelanin** - red-yellow soluble polymer formed by the conjugation of cysteine or glutathione (Slominski A *et al.*, 2004).

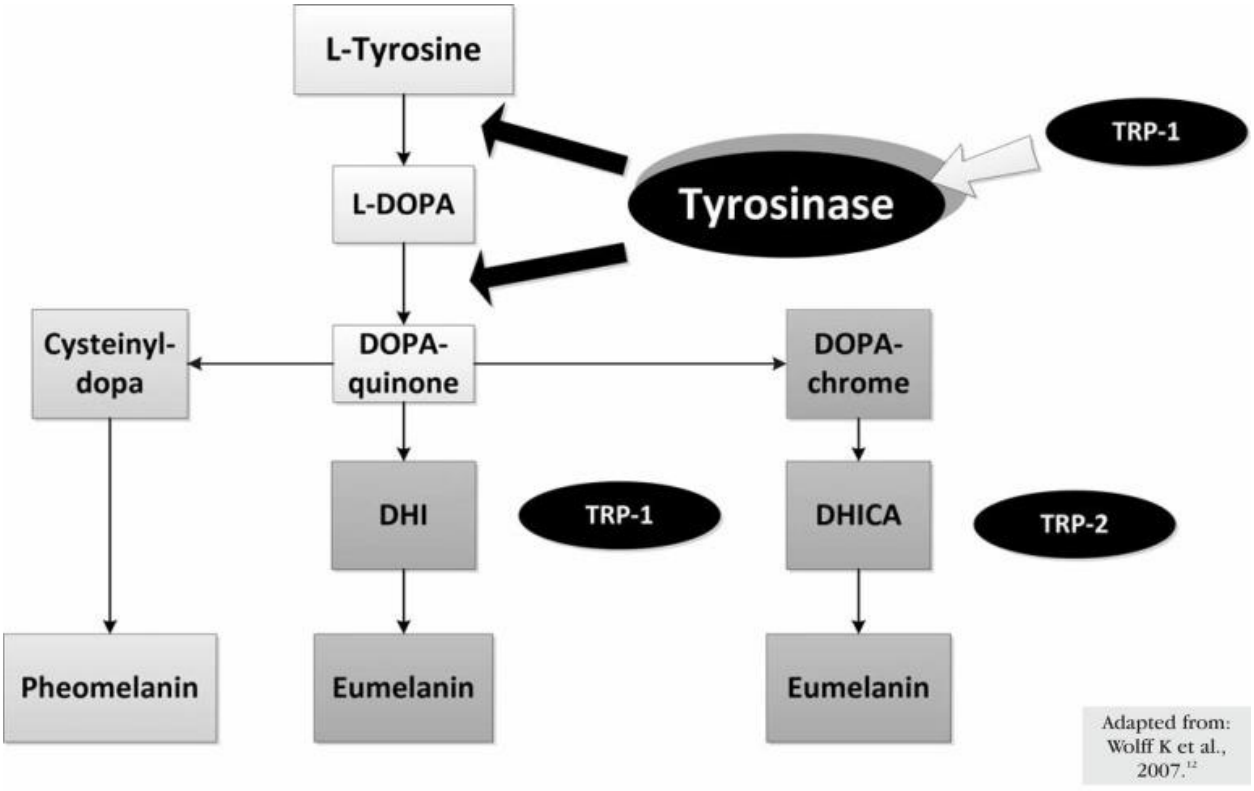

Figure 2: Synthesis of the two types of melanin and representation of the functions of the major enzymes involved in melanogenesis

The first and rate-limiting step in melanogenesis is the conversion of L-tyrosine to DOPA (Dihydroxyphenylalanine) catalysed by tyrosinase. Tyrosinase is regulated by the transcription factor named **MITF**. DOPA then, undergoes oxidation to form dopaquinone which is immediately converted into dopachrome and then to DHI (5, 6 dihydroxy indole). Also tyrosinanse related protein 2 (TRP 2) converts dopachrome to dihydroxy indole carboxylic acid (DHICA). Further, DHI and DHICA polymerize to form eumelanin. Cysteine/glutathione reacts with the dopaquinone

to produce cysteinyldopas that may undergo further cyclization to benzothiazines and higher condensates giving rise to pheomelanins. (Taieb 2000; Simon, Peles *et al*., 2009; Denat *et al*., 2014)

Melanin production is triggered by ultraviolet rays present in sunlight. UVR fall on the epidermal layer consisting of keratinocytes which activates the p53 tumor suppressor protein. Activation of p53 in keratinocytes increases the expression of POMC peptides (Cui, Widlund *et al*., 2007). POMC is a strong precursor of melanotrophic peptides α-melanocyte-stimulating hormone (α-MSH) and adrenocorticotrophic hormone (ACTH). α-MSH are secreted by keratinocytes and then competitively bind to melanocortin 1 receptor (MC1R) on the melanocyte which in turn activates the cell-signalling pathways, including the cyclic adenosine monophosphate (cAMP)-dependent protein kinase pathway and the mitogen-activated protein (MAP) kinase pathway. In addition to it, induction of cyclic AMP production leads to phosphorylation of cAMP responsive-element-binding protein (CREB) transcription factor family members. (Videira, Moura *et al*., 2013)

CREB, in turn, transcriptionally activates various genes, including that encoding microphthalmia transcription factor (*MITF*), which is a transcription factor, pivotal to the expression of numerous pigment enzymes such as tyrosinase (TYR, enzyme involved in rate limiting step of melanogenesis) and differentiation factors. MITF transcriptionally activates the pigmentory enzymes which is then transported into melanosomes, site for melanin production (Levy, Khaled *et al.*, 2006; Park, Kosmadaki *et al*., 2009).

Melanocytes are highly dendritic and are in contact with the neighboring keratinocytes as mentioned above. Each melanocyte is in contact with approximately 36 keratinocytes. Melanosomes containing the melanin migrate from the center of the melanocyte cell body to the end of the dendrites and are deposited into keratinocytes. (Shajil, Chatterjee *et al.*, 2006). The melanosomes accumulate in the keratinocytes and form a shield of melanin. Melanin is therefore the most important photoprotective factor considered as a broadband UV absorbent which provides protection to the skin against ultraviolet radiation from sunlight, along with it has antioxidant and radical scavenging properties (Swalwell *et al*., 2012).

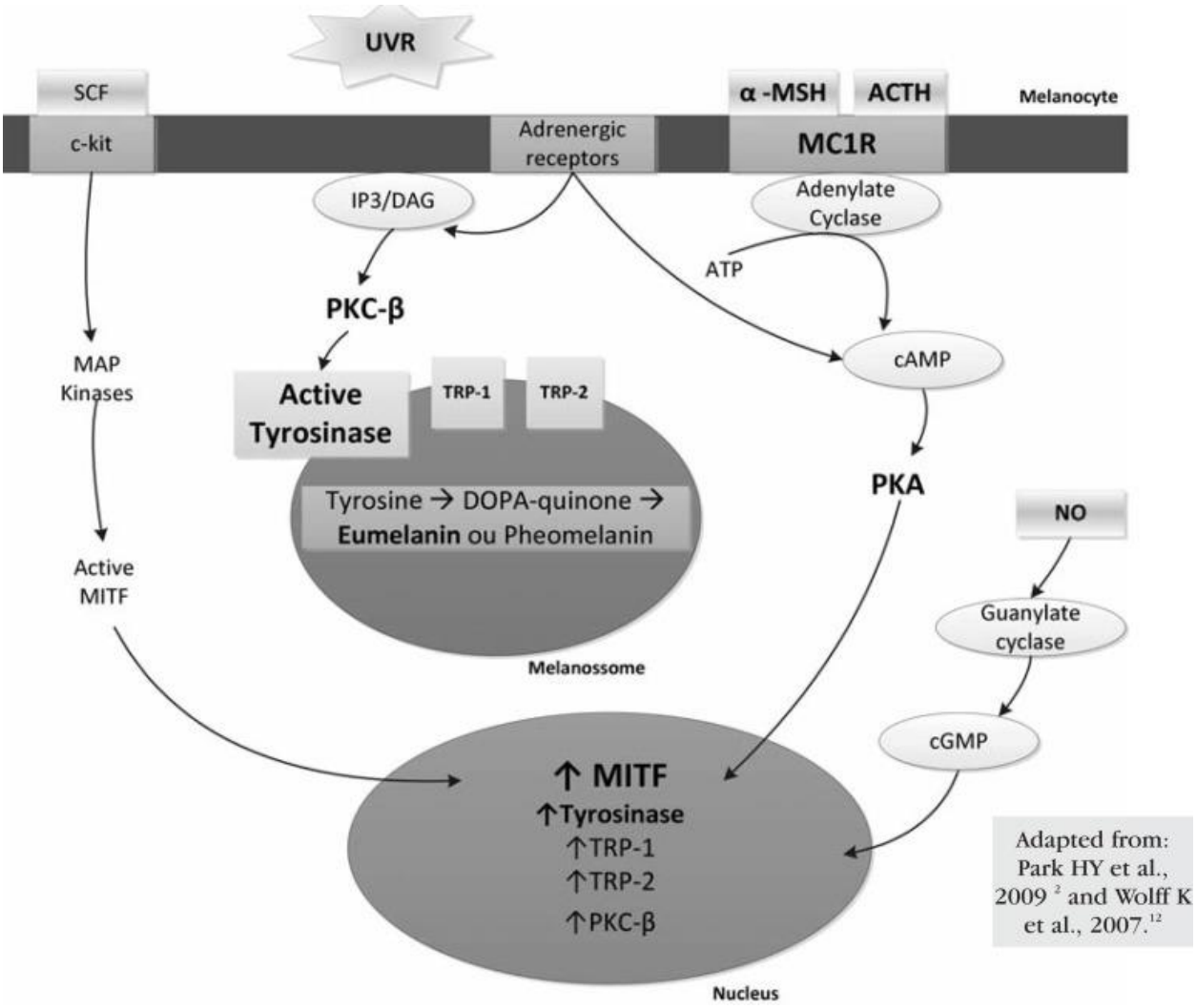

Figure 3: Melanocyte role and representation of the different signaling pathways regulating melanogenesis: activation factors, receptors, second messengers, and melanogenic enzymes

2.3 VITILIGO

Vitiligo is a chronic stigmatizing disease, which mainly affects melanocytes from epidermis, leading to the development of white (depigmented) patches on the skin. Its estimated prevalence is 0.5% worldwide (Allam M *et al.*, 2013). These lesions can appear in different shapes and sizes and may be present in any area of the body. So far, the origin of vitiligo has not been traced and the pathogenesis is complex, involving the interplay of a multitude of variables. Although there is no treatment that ensures the complete cure of the disorder, there are some pharmacological, phototherapy, and surgical therapies available (Bhagwat M. 2010). Several theories have been proposed so far to unravel the pathogenesis of vitiligo such as autoimmune theory, autocytotoxic theory, the neural theory, and 'impaired epidermal cytokine' theory which are considered to be involved in determining this disease.

CLASSIFICATION

According to the review conducted by the *Vitiligo Global Issues Consensus Conference* between 2011-2012, vitiligo can be classified in the following clinical forms:

Table 1: Classification of Vitiligo

Type	Traits
Segmental vitiligo Also called: ▪ Unilateral vitiligo	▪ Appears on 1 segment of the body, such as a leg, face or arm. ▪ About half of people lose some hair color, such as on the head, an eyelash or an eyebrow. ▪ Often begins at an early age. ▪ Often progresses for a year or so then stops.
Non-segmental vitiligo Also called: ▪ Bilateral vitiligo ▪ Vitiligo vulgaris ▪ Generalized vitiligo	▪ Most common type. ▪ Appears on both sides of the body, such as both hands or both knees. ▪ Often begins on hands, fingertips, wrists, around the eyes or mouth, or on the feet. ▪ Often begins with rapid loss of skin color, which then stops for a while. Color loss often starts up later. This start-and-stop cycle usually continues throughout a person's lifetime. ▪ Color loss tends to expand, growing more noticeable and covering a larger area.

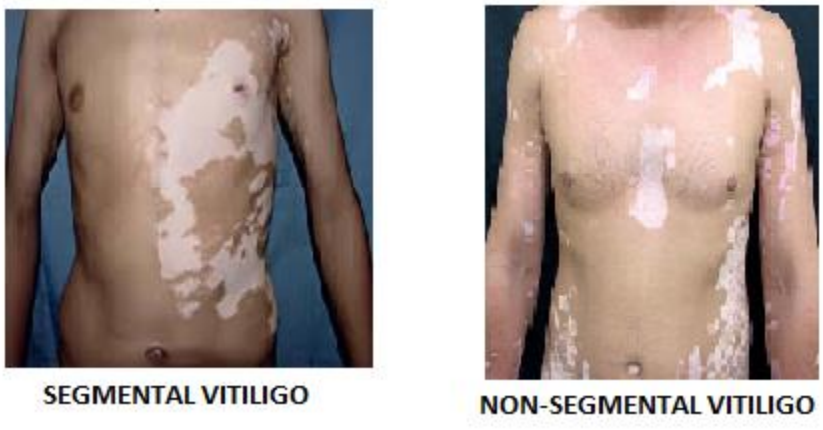

Figure 4: Depiction of different types of vitiligo (Faria A.R., *et al*., 2014)

EPIDEMIOLOGICAL ASPECTS

The disease does not discriminate between genders, age groups or skin colors. The exact cause remains unknown. (Kruger C. *et al*., 2015). It can appear at any age, and the average age of onset is somewhat variable in different geographic regions (Majumder P.P. *et al*., 1993). The mean age ranging from 22 years in the U.S. and India, 24 in Brazil and 25 years old in England (Allam M *et al*., 2013).

Vitiligo is commonly present in children, with half of all cases developing before 20 years of age. Although studies have characterized differences between pediatric and adult vitiligo, very little is known about vitiligo presenting in early childhood (Mu E.W. *et al.*, 2015).

CLINICAL DESCRIPTION

In accordance to the clinical picture, one or more well demarcated and white maculae, progressing in size and number are seen in the patients, which are asymptomatic generally. The lesions usually appear on sun exposed or constitutionally hyper-pigmented areas or on sites of stretch and pressure (face, dorsum of hands and fingers, external genitalia, knees and elbows). Rarely an inflammatory border may be found around the vitiligo patch resulting in a raised and erythematous edge (inflammatory vitiligo).

2.4 VITILIGO PATHOGENESIS: ETIOLOGICAL THEORIES

The exact origin of vitiligo is still unclear, and the pathogenesis is dependent on multiple factors. (Schallreuter, K. U. *et al*., 2008). There is a multifactorial genetic component predisposing certain individuals to vitiligo and family history is a variable found in approximately one-third of the people with the disease (Whiton M. E. *et al*., 2015). There is also strong genetic evidence of a link between vitiligo and other autoimmune diseases (Spritz, R.A. 2013).

Various theories were postulated explaining the destruction of melanocyte at the lesional site, causing depigmentation. (Lerner *et al.,* 1959) in the 1950's firstly proposed the neural theory, and after that, model of reactive oxygen species (ROS), the autoimmune hypothesis and the melanocytorrhagy hypothesis have appeared. But none of these hypothesis could explain the entire spectrum of the disorder. The current thought is that vitiligo represents a group of heterogeneous pathophysiologic disorders with a similar phenotype (Alikhan, A. *et al*., 2011). The convergence theory states that stress, accumulations of toxic compounds, infection, autoimmunity, mutations, altered cellular environment, and impaired melanocyte migration can all contribute to the pathogenesis (Le Poole, I.C. *et al.,* 1993).

NEUROCHEMICAL THEORY

According to the neural theory, segmental vitiligo favors dysfunctioning of the sympathetic nervous system and disturbs melanin production which leads to depigmentation (Mohammed, G. F *et al*., 2015). In simple words, neurochemical hypothesis suggests that release of neurochemical factor such as norepinephrine and acetylcholine from the peripheral nerve endings destroys the melanocyte or inhibits melanin production giving rise to depigmentaion spot and thus contribute to vitiligo pathogenesis. (Shajil, Chatterjee, *et al*., 2006; Panja, Bhattacharya, *et al.,* 2013)

High concentration of neurochemical may arise due to both genetic and non-genetic factors. High concentration of norepinephrine and its metabolite in vitiligo patients may be due to a reduction in phenylethanolamine-N-methyl transferase(PNMT) activity and subsequent increase in tyrosine hydroxylase (TH) activity. These enzymes play a key role in production of L-DOPA from L-tyrosine. Also, increased activity of TH enzyme is due to decreased 4a-hydroxy-6BH4 dehydratase (DH) activity in vitiligo patients (Schallreuter, Wood, *et al*., 1994). Increased level of norepinephrine also appears to induce another catecholamine degrading enzyme, monoamine

oxidase (MAO) (Bindoli, Rigobello, *et al.*, 1992). Keratinocyte and melanocyte in the depigmented skin exhibit increased monoamine oxidase-A activity which further causes keratinocytes to produce 4-fold more norepinephrine and 6.5-fold less epinphrine that control keratinocytes (Schallreuter, Wood, *et al*., 1996).

OXIDATIVE STRESS THEORY

Both lesional and non lesional skin of vitiligo has abnormal low level of catalase enzyme, which correlates with high H_2O_2 levels throughout the epidermis.(Schallreuter, K.U. *et al.,* 1991, Schallreuter, K.U.*et al*., 1999) A single nucleotide variant in the catalase gene may interfere with the enzyme's subunit assembly and function, and is seen more frequent among vitiligo patient (Casp, C.B. *et al*., 2002).Reactive oxygen species (ROS) and H_2O_2 in excess can damage biological processes through oxidative mechanisms with limited ability for repair due to H_2O_2 excess accounting the damage, and this situation has been documented in vitiligo patients. The resultant protein and lipid damage could be sufficient with its own to initiate melanocytic failure, but another effect of oxidation could be to initiate melanocyte failure and apoptosis leading to uptake by Langerhans cells or DCs and if these Langerhans cells or DCs become activated, they may trigger melanocytes reactive immune response that can eradicate melanocytes in the skin leading to depigmentation. This immune response principally involves cytotoxic T-cells (Glassman S.J. 2011). In addition to the failure of the regulatory T cell mechanisms that was mentioned earlier allows the process to continue indefinitely, in keeping with the chronic, relentless course of generalized vitiligo (Schallreuter, K.U.*et al*., 1994, Klarquist, J. *et al.,* 2010).

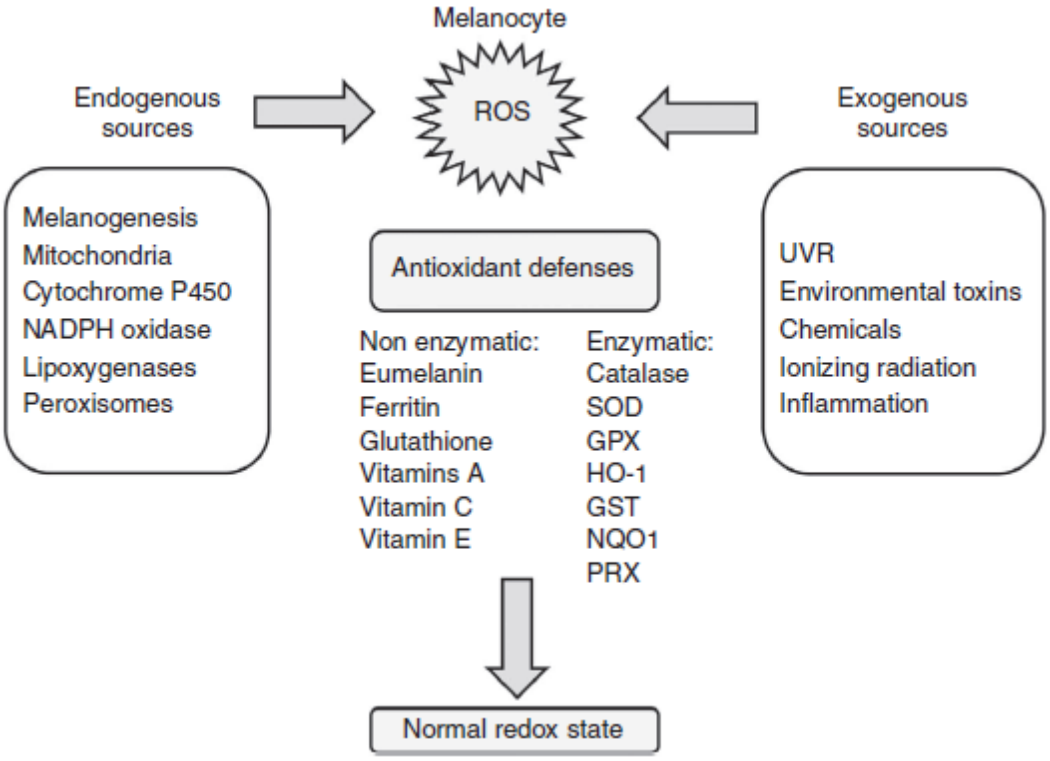

Fig 5: Induction of reactive oxygen species (ROS) by endogenous and exogenous sources and antioxidant defenses that restore normal redox state in melanocytes. (Denat, Kadekaro, *et al.*, 2014)

AUTOIMMUNE THEORY

Although the etiology of Vitiligo remained obscure, the earliest evidence relating to the genetic basis of vitiligo was the 1855 description by Addison, of a patient with idiopathic adrenal insufficiency (Addison's Disease), generalized vitiligo (GV) and pernicious anemia (Colucci, R. *et al.*, 2014). Over the next years, several studies have been reported showing concomitant occurrence of multiple autoimmune diseases with GV (Garcia-Melendez, M.E. *et al.*, 2014).

The frequencies of six autoimmune disorders were significantly elevated in vitiligo patients and their first-degree relatives such as vitiligo itself, autoimmune thyroid disease (particularly hypothyroidism), pernicious anemia, Addison's disease, systemic lupus erythematosus (SLE), and probably inflammatory bowel disease (Kohro, T., *et al.*, 2000) (Kumar, R., *et al.*, 2012), highlighting a causal connection among autoimmune diseases occurring altogether.

Modern genetic studies of vitiligo have principally entailed five scientific approaches: genetic linkage analysis of families with multiple affected relatives (multiplex families), candidate gene association studies comparing relatively small numbers of vitiligo patients (cases) to unaffected controls, genome-wide association studies (GWAS) comparing far larger numbers of cases to controls, DNA sequencing studies and gene expression studies (Huang, Y. *et al*., 2103). Several genes have been identified with the help of such genetic studies. Vitiligo susceptibility genes such as HLA, PTPN22, NLRP1, XBP1 via candidate gene association and gene expression studies, have been confirmed susceptible to vitiligo, all encode important immunoregulatory proteins, favoring the autoimmune hypothesis of GV pathogenesis. (Laddha, N.C. *et al*., 2012). Three genome wide association studies (GWAS) of GV have been reported, one from European-derived white population (Lu, L. *et al.*, 2014) and the other from China (Marín-Martín, F.R. *et al*., 2014). Together these studies have identified 17 genes confirmed for GV susceptibility. To name, the identified GV susceptible loci include *SMOC2* (SPARC-related modular calcium binding 2), *HLA* class I (specifically, *HLA-A**0201), *HLA* class II, *PTPN22*, *RERE* (arginine-glutamic acid dipeptide repeats), *FOXP1* (forkhead box P1), *LPP* (LIM domain containing preferred translocation partner in lipoma),*CCR6* (chemokine (C-C motif) receptor 6), *IL2RA* (interleukin 2 receptor, α), *TYR*, *GZMB* (granzyme B),*NLRP1*, *UBASH3A* (ubiquitin-associated and SH3 domain containing A) and *C1QTNF6* (C1q and tumor necrosis factor related protein 6), *TSLP* (thymic stromal lymphopoietin), *XBP1* and *FOXP3* (forkhead box P3) (Laddha, N.C. *et al*., 2012).Virtually all of the confirmed GV susceptibility loci have been known to encode immunoregulatory proteins, and many have been associated with genetic susceptibility to other autoimmune diseases that are epidemiologically linked to GV (Laddha, N.C. *et al*., 2012). Out of these genes, TYR, which encodes tyrosinase, the key enzyme for melanin biosynthesis in melanocytes, is an exception in such a way that beyond its role in pigmentation, it acts as a major autoantigen in GV. This indicates the analogous behavior of GV to type 1 diabetes and autoimmune thyroid disease, in that genetic susceptibility to disease involves genes that encode key specialized intracellular components of the autoimmune target cell types and that constitute major autoantigens for the corresponding disease (GV: *TYR*, tyrosinase; type 1 diabetes: *INS*, insulin; autoimmune thyroid disease: *TG*, thyroglobulin) (Laddha, N.C. *et al.*, 2012).

Table 2: List of some other autoantigens (Laddha, N.C. *et al*., 2012)

Autoantigen	Function
Tyrosinase	Melanogenic enzyme
TRP-2	Melanogenic enzyme
TRP-1	Melanogenic enzyme
Pmel-17	Melanocyte-specific protein
MCHR1	Melanin concentrating hormone receptor 1
SOX 9	Transcription factor
SOX 10	Transcription factor

With regard to this autoimmune theory, additionally, the involvement of humoral and cell mediated immune responses have been documented by the following studies (Mehaney, D.A. *et al*., 2014). Finding of circulating autoantibodies directed towards melanocyte antigens support the hypothesis that vitiligo is an autoimmune disease mediated by an immune reaction to pigment cells (Spritz, R.A. 2010). Also peripheral blood of patients with vitiligo is also characterized by high frequencies of melanocyte-reactive cytotoxic T cells (Spritz, R.A. 2013).

NLRP1 is a regulator of the innate immune response (Martinon, F. *et al*., 2007) and is expressed in many immunocompetent cell types, particularly the Langerhans cells of the skin (Kummer, J.A., *et al*., 2007). Surface Toll-like receptors (TLRs) are being stimulated by pathogen- or damage-associated molecular patterns with subsequent assembly of the NLRP1 inflammasome and activation of caspase-1, which then cleaves the inactive IL-1β precursor (pro–IL-1β) to the mature bioactive IL-1β, thereby stimulating downstream inflammatory responses (Dinarello, C.A. 2011). The predominant *NLRP1* multivariant haplotype associated with common autoimmune diseases up-regulates IL-1β processing via the NLRP1 inflammasome, as studied in vitiligo patients.

The proinflammatory cytokine IFN-*γ* levels were noted to be significantly elevated in vitiligo patients compared to healthy controls (Ala Y. *et al*., 2015). IFN-γ indirectly increases the expression of intercellular adhesion molecule-1 (ICAM-1) on melanocytes and enhances T-cell – melanocyte attachment in the skin and thus establishes a link between cytokine and t-cell mediated destruction of melanocytes in vitiligo (Ala, Y.*et al*.,2015) (al Badri, A.M. *et al*., 1993)

Additionally, a significant difference was found in the mean serum concentrations of the anti-inflammatory cytokine IL-10 between patients and controls (Ala, Y., *et al*., 2015). It has been reported that in vitiligo individuals, there is high levels of IFN-γ:IL-10 ratio which indicates the lower levels of CD4+/CD8+ T-cells.

Dwivedi, M. *et al* (2013) proposed that two variants from *IFNG* CA microsatellite (12 CA repeat) but not +874A/T may be a genetic risk factor for GV in Gujarat population; however, +874T allele may play a role in increased expression of *IFNG* mRNA and protein levels which could affect the onset and progression of the disease.

In addition to CD8(+) cell-mediated melanocyte destruction in autoimmune vitiligo a complex Th17 cell-related cytokine environment influences the local depigmentation (Kotobuki, Y. *et al*.,2012). Cytokine IL-17, found in epidermis of active vitiligo, is able to induce the release of proinflammatory cytokines (namely, IL-1, IL-6, TNF*α*, TGF*β*, GM-CSF, and prostaglandins) from activated immune cells such as fibroblasts, keratinocytes, endothelial cells, and macrophages (Kotobuki, Y. *et al*., 2012) (Colucci, R. *et al.,* 2015).

MELANOCYTORRHAGY HYPOTHESIS

This hypothesis proposes that melanocytes are weakly anchored and a minor friction and/or other stress can induce upward migration and loss of melanocytes (Gauthier, Y. *et al*., 2003) and this theory is considered to be of relevance in Koebner phenomenon and vitiligo lesions over trauma sites. Melanoctytorrhagy explains that melanocyte with defective adhesion system along with altered melanocyte responses to friction and possibly other types of stress, induces their detachment and subsequent trans epidermal loss is foreseen. Detachment and trans epidermal elimination of melanocytes following minor trauma such as stress, accumulation of ROS are probably the cause of depigmentation, known as Koebner phenomenon. (Kumar, R.*et al.,* 2012) Tenascin, an extracellular matrix molecule which inhibits adhesion of melanocytes to fibronectin, is elevated in vitiligous skin, and may contribute to loss of melanocytes or ineffective population. (Le Poole, I.C. *et al*., 1997).

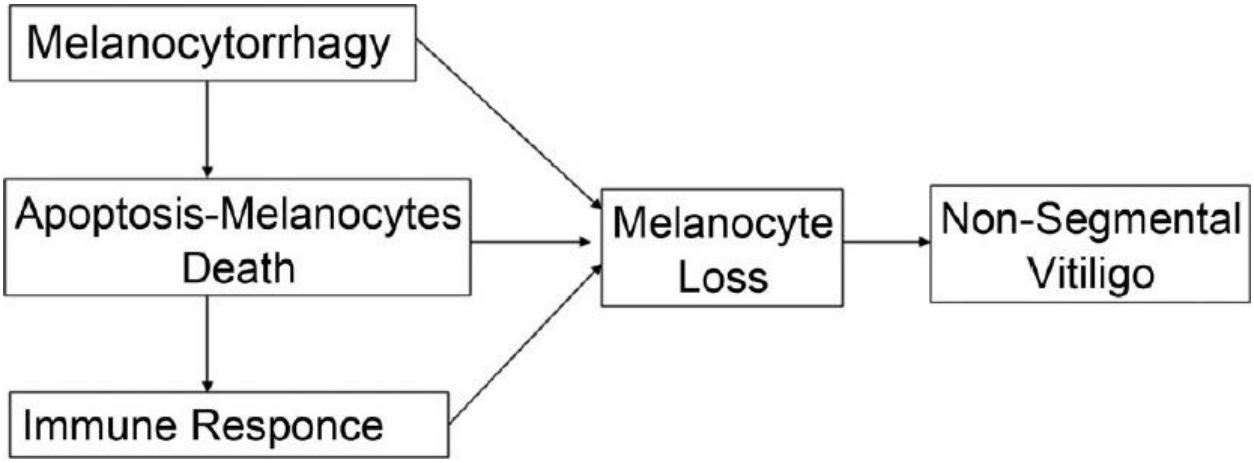

Figure 6: Depicting interconnections between melanocytorrhagy, apoptosis, and immune response, leading to melanocyte loss in non-segmental vitiligo (Kumar, R.*et al.,* 2012).

The baseline expression of adhesion molecules may differ in vitiligo patients as compared to controls, as melanocytes are poorly attached to the basement membrane as compared to keratinocytes. Melanocytes adhesion, spreading, and migration are mediated by integrins, whereas the interactions between melanocytes and keratinocytes are mediated by cadherins. (Hara, M. *et al*.,1994)

Adhesion of melanocytes is also affected by the levels of endothelin-1(Jamal, S. *et al*., 2002). In vitro melanocyte attachment to laminin is mediated primarily by a6b1 integrins. E-cadherin is the major mediator of human melanocyte adhesion to keratinocytes in vitro. Melanocytes dendrites have a very crucial role in the adhesion, migration, and melanosome transfer. In human skin, one melanocyte makes contact with several keratinocytes with the help of dendrites. Integrins that help in dendrite formation are located preferentially along or at the tip of dendrites, whilst integrins that mediate attachment tend to localize over the cell body as well as along the dendrites (Hara, M. *et al*., 1994).

Recently, it has been shown that in unstable vitiligo patients, melanocytes were poorly attached to Type IV collagen, whereas stable vitiligo melanocytes and control melanocytes were firmly adhered to Type IV collagen. (Kumar, R. *et al*., 2011).

NEW HYPOTHESIS: A DISORDER OF MELANOCYTE SURVIVAL

The active mechanism by which the melanocytes are destroyed is not being determined yet. Several morphological observations suggest that the involvement of melanocyte apoptosis and of another SCF/c-kit/MITF/Bcl-2 pathway in the pathogenesis of vitiligo as this pathway plays a key role in the survival of melanocytes. SCF from keratinocyte origin protects melanocytes from TNF-related apoptosis inducing ligand(TRAIL) (Beazley, W.D. *et al*., 1999). Bcl-2, a MITF- dependent kit transcriptional target in melanocytes is essential for the maintenance of lifetime of melanocytes (McGill, G. G., *et al.,* 2002).

Therefore, a decrease in the expression of Bcl-2, increases the susceptibility of melanocytes towards apoptosis (van den Wijngaard, R.M. *et al.*, 2000).

In conclusion, single hypothesis cannot explain all the various clinical type of vitiligo but they do work in combination such as onset of oxidative stress act as a trigger to cause the autoimmunization which leads to melanocyte loss. It has been speculated that local systemic factors affect the homeostasis of the epidermal melanin unit in segmental vitiligo whereas an impaired redox status of the epidermal melanin unit acts as the trigger further leading to inappropriate immune response in non-segmental vitiligo. The neural theory is more related to segmental vitiligo whereas the autoimmune theory is involved in non-segmental vitiligo (Anbar Tel, Abdel-Raouf, *et al.,* 2011).

2.5 GENETICS OF VITILIGO

Researchers from different areas of the world explored intensively the possible shared susceptibility genes involved in vitiligo and other autoimmune diseases and additional genes that may mediate the vitiligo itself. Four different approaches have been used as mentioned earlier also, to identify genes that mediate the susceptibility to vitiligo: gene expression analyses, candidate gene association studies, genome-wide linkage studies and genome wide association studies (GWASs). Gene expression studies in vitiligo were done to analyze the changes in the expression pattern of several genes associated with immunomodulation, melanogenesis, and regulation of the development and survival of melanocytes.

The inheritance of vitiligo cannot be explained by simple Mendelian pattern. It is a polygenic disease characterized by multiple susceptibility loci, genetic heterogeneity and incomplete penetrance with gene-gene and gene-environment interactions. Recently, a number of genes which play a role in vitiligo susceptibility, including *HLA*, *PTPN*22, *NALP*1, *XBP*1, *FOXP*1, *IL*2RA have been tested for genetic association with vitiligo.

It has been reported that *TNF-α* −238, −308, −857, −863 and −1031 promoter polymorphisms are significantly associated with Gujarat vitiligo patients. It thus, suggests the important role of TNF-α in pathogenesis of vitiligo. Vitiligo patients showed significant increase in *TNF*-α transcript and protein levels as compared to controls suggesting that melanocyte death in patients could be triggered due to the increased TNF-α levels. (Laddha, N.C. *et al*., 2012)

The *PTPN22* gene encodes for a lymphoid protein tyrosine phosphatase, a regulator of the activation and development of T-cells. This study analyzed the genotype distribution and allele frequency for *PTPN22 +1858C/T* polymorphism corresponding to codon 620 (620Arg-Trp) and has been found associated with active Vitiligo. (Colucci, R. *et al*., 2015).

Table 3: Genes involved in Vitiligo susceptibility

GENE	MAPPING	PRODUCT	DISEASE
PTPN22	1p13	Lymphoid protein tyrosine phosphatase	Vitiligo vulgaris
FOXD3	1p32-p31	Transcription factor involved in melanocyte differentiation	Early and progressive Vitiligo
VIT1/FBX011	2p21	?	Vitiligo vulgaris
CTLA4	2q33	Antigen 4 of T- cytotoxic lymphocytes	Vitiligo vulgaris
MITF	3p14.1-p12.3	Transcription factor	Vitiligo vulgaris
KIT	4q12	Transmembrane tyrosine kinase	Vitiligo vulgaris
MHC (HLA-DRB1, HLA-DRB4,HLA-DQB1)	6p21.1	Major MHC	Vitiligo vulgaris
ESR1	6p25.1	Oestrogen receptor 1	Vitiligo vulgaris
CAT	11p13	Catalase	Vitiligo vulgaris
GTPCH (GTP-cyclohydroxylase I gene)	14q22.1-q22.2	Rate limiting enzyme of tetrahydrobiopterin pathway	Vitiligo vulgaris
ACE	17q23	Angiotensin converting enzyme	Vitiligo vulgaris
AIRE	21q22.3	Transcription factor	APECED
COMT	22q11.2	Catecholamine O methyl transferase	Vitiligo vulgaris

Source: Spritz, R.A. (2006).

Recently, role of Liver X Receptor (LXR) in skin physiology and pathology has evolved rapidly because of their role in epidermal proliferation, carcinogenesis, differentiation and permeability barrier function, which identifies them as promising drug targets for the treatment of skin diseases (Kumar, R. *et al*., 2012).

2.6 Liver X Receptor Gene:

Liver X Receptor (LXR-alpha/ NR1H3 and LXR-beta/ NR1H2) are ligand (such as oxysterols, high concentrations of D-glucose and phytosterols) activated nuclear transcription factors which regulate the expression of target genes involved in lipid biosynthesis, cholesterol homeostasis, immunity and inflammation (Jamroz-Wisniewska, Wojcicka, *et al*., 2007). Oxysterol (eg 22(R)-hydroxy cholesterol (22 (R)-HC), 24(S), 25-epoxycholesterol (24(S), 25-EC)) are the natural ligand of LXR enzyme which are either intermediates in cholesterol biosynthesis or originate by the oxidation of cholesterol by various cytochrome P450 (CYP) isoforms.

LXRs contain a central DNA-binding domain consisting of a zinc-finger module and a large ligand-binding domain with a lipophilic core that binds specific small-lipid molecules such as oxysterol. After ligand binds, nuclear receptors undergo a conformational change that promotes interaction with retinoid X receptor. This heterodimer binds to the LXR response element (LXRE) which usually consists of direct repeats of the hexamer AGGTCA, separated by four nucleotides (DR4). Thus, LXRs regulate gene expression through binding to DNA as heterodimers with the retinoid X-receptor (RXR) (NR2B1) (Chen, Li *et al.*, 2008).

Gene view

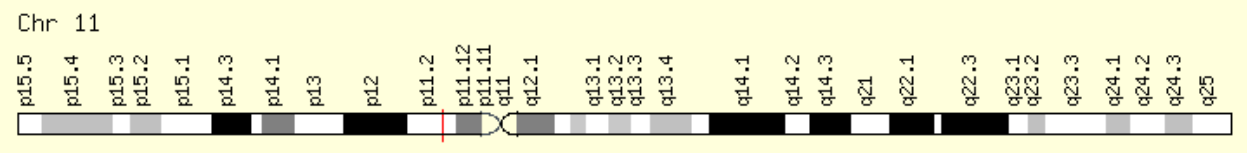

Figure 7: NR1H3 Gene in genomic location

(Source: http://www.genecards.org/cgibin/carddisp.pl?gene=NR1H3&snp=494&search=nr1h3#snp)

Gene summary

Chromosome location: Ch11 (p11.2)

Gene size: 20,734 bases

Orientation: Plus strand (+)

Exon count:16

Number of transcripts: 35

Selected transcript: variant 2

Gene product: protein isoform 2 [length-387 amino acids]

Structural information: Crystal structure of the LXRalfa - RXRbeta LBD heterodimer with PDB id: 1UHL

Originally, Liver X Receptor considered as "orphan" nuclear receptors, because their natural ligands were unknown following the discovery of oxysterols as their natural ligands which bind to and activate these receptors at physiological concentrations (Willy, Umesono *et al.,* 1995), they have been removed from orphan category. Since their expression and function is high in liver, they been named as Liver X Receptor.

LXR exists in two isoforms: LXR-alpha and LXR-beta. LXR-alpha is highly expressed in several metabolically active tissues, such as liver, intestine, adipose tissue, and macrophages, whereas LXR-beta is ubiquitously expressed in most tissues (Steffensen and Gustafsson 2004; Lee, Park *et al.,* 2013). Both isoforms are activated by endogenous oxysterol.

LXR are also found to be expressed in the skin tissues such as sebaceous glands, hair follicle, epidermal keratinocyte and fibroblast (Billoni, Buan, *et al.*, 2000; Russell, Harrison, *et al*., 2007). They found to have role in skin physiology and pathology such as proliferation, carcinogenesis, differentiation and permeability barrier function (Kumar, R. *et al.,* 2012). LXR activation induces keratinocyte differentiation and inhibits proliferation (Komuves, Schmuth, *et al.*, 2002). LXR induces lipid synthesis in sebocytes and inhibits the expression of cytokines and metalloprotinases in skin–photoaging models. (Kumar, R. *et al.,* 2012) Marked expression of LXRs in skin speculate

that it might have an important role in pathogenesis of skin disorders such as psoriasis, acne vulgaris, vitiligo etc.

LXR activator exhibits potent anti-inflammatory activities in many inflammatory disorders including dermatitis, artherosclerosis and pulmonary inflammation through the suppression of several NF- kappa B target genes such as MMP 9, CCL2, CCL7, IL-1β and cyclooxygenase-2 (Bensinger, and Tontonoz 2008).

The function and characteristics of LXRs in skin have been recently widely studied but their expression and function in relation to melanocyte have not yet been investigated. Recently, Kumar et.al.(Kumar, Parsad *et al.*, 2010) demonstrated that LXRs are also expressed in melanocytes. Kluger et.al.(Kluger, Cotton, *et al.*, 2008) reported a marked expression of LXR-alpha in cells adjacent to dermal papilla, speculating that it may correlate with the site of hair melanocytes. Important genes involved in regulation of melanocytes such as MITF, MMPs, certain inflammatory genes such as IL-6, IL-1beta are target genes of LXR which suggest that LXRs might be playing a role in regulation of melanocyte and melanogenesis (Lee, Park *et al.*, 2013).

Recently, Kumar et.al.(Kumar, Parsad *et al.*, 2010) demonstrated that LXR-alpha are upregulated in the melanocytes from perilesional skin as compared to the normal skin of vitiligo patient suggesting its role in vitiligo pathogenesis

Role of LXRs in Pathogenesis of Vitiligo

Study by Kumar *et.al.*(Kumar, Parsad *et al.,* 2010) demonstrated that expression of liver X receptor-alpha (LXR-α) at both mRNA and protein level was significantly higher in perilesional skin as compared to the normal skin of vitiligo patient. Further, they have demonstrated that on treating control melanocytes with LXR-α agonist 22-hydroxy cholesterol, the adhesion of melanocytes to type IV collagen and laminin 5 decreases significantly. Increase in LXR-α expression might decrease the cell adhesion molecule, which ultimately leads to the detachment of melanocytes from the basement membrane in perilesional vitiligo skin which can ultimately lead to Melanocytorrhagy (Kumar R. *et al*., 2012). In addition to it, our previous study provides an evidence that the LXR-α −6A and +1257T alleles contribute to risk of vitiligo in North Indian population and highlight the importance of this gene in the vitiligo pathogenesis (Agarwal S. *et al*., 2016).

Study by Lei *et.al*.(Lei, Vieira *et al.*, 2002) demonstrated that MMP 2 plays an important role in melanoblast migration from the border of vitiligo lesions into clinically depigmented epidermis which is crucial for the repigmentation of vitiligous skin. Additionally, study by Kumar *et.al.(*Kumar, Parsad *et al., 2011)* reported that MMP-2 and MMP-9 are downregulated in vitiligo patient and further, it was shown that LXR-α gene knock-down significantly increases the expression of MMPs. Thus, high expression of LXR-alpha might be contributing to the inhibition of MMPs because of which melanoblast are not able to migrate at the basal layer of the epidermis. No repigmentation is observed as a phenomenon.

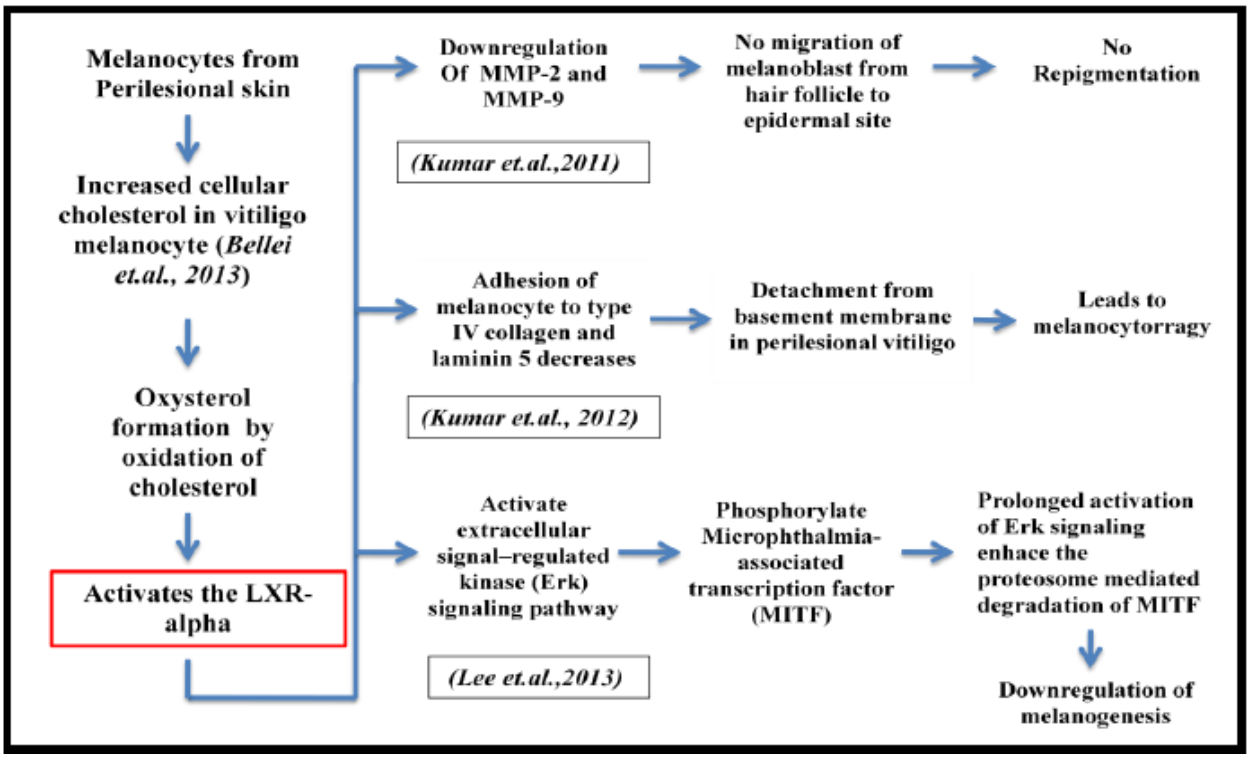

Fig 8: Role of LXR-alpha in vitiligo pathogenesis

Thus, Higher expression of LXR-α in perilesional skin melanocytes significantly decreases the adhesion, proliferation and matrix metalloproteinases and increases apoptosis. Based on all these studies LXRs appear to have important role in vitiligo pathogenesis and considered as a potential therapeutic target for vitiligo.

This project is being focused on the genetic variants responsible for the alteration of gene expression. Therefore, significantly predicted nsSNPs are genotyped to elucidate any association between the LXR-alpha SNP with vitiligo susceptibility.

2.7 SINGLE NUCLEOTIDE POLYMORPHISM

Nonsynonymous single nucleotide polymorphisms (nsSNPs) are single base changes in coding regions that cause an amino acid substitution in the correspondent proteins. These missense variants constitute the most identifiable group of SNPs represented by a small (<1%) proportion (Marín-Martín, F.R. *et al*., 2014).

The nsSNPs might alter structure, stability, and function of proteins and produce the least conservative substitutions with drastic phenotypic consequences (Yates C.M. *et al*., 2013) (Rodriguez-Casado, A. 2012).

Approximately 206 nsSNPs have been reported for LXR-α gene, out of which I39V (rs11545529) and R355Q (rs61731956) variants of LXR-α gene have been selected to experimentally validate their role in introducing alterations in the protein stability as suggested through computational analysis. Thus, these two variants are further genotyped by PCR-RFLP to asses any association with vitiligo susceptibility.

- **rs11545529 (+10906 A*>G)**
    - A to G transition at position 10906 which is downstream to ATG site
    - Ancestral allele: A
    - Location: Chromosome 11:47259862 (forward strand)
    - Exon position: exon 3

Functional characteristics

The location of this variant in the genome signifies its role in the final protein structural conformation and its subsequent functionality. +10906 A>G polymorphism tends to change the amino acid isoleucine at position 39 in the protein sequence, to valine. This amino acid change could produce structural and functional alterations to the gene product, which could ultimately hamper the basic function of this protein.

- **rs61731956 (+19640 G*>A)**
    - G to A transition at position 19640 which is downstream to ATG site
    - Ancestral allele: G
    - Location: Chromosome 11:47268596 (forward strand)
    - Exon position: exon 9

Functional characteristics

The location of this variant in the genome signifies its role in the final protein structural conformation and its subsequent functionality. +19640 G>A polymorphism tends to change the amino acid arginine at position 355 in the protein sequence, to glutamine. The change in the polarity of these two amino acids could produce structural and functional alterations to the gene product.

Through previous studies, no association of these two polymorphisms with any disease, have been found yet.

Table:4 Location and details of nsSNPs

Polymorphism reference no.	**Nucleotide Change**	**Amino Acid change**	**Exon**
rs11545529	A/G	Ile 39 Leu	3
rs61731956	G/A	Arg 355 Gln	9

2.8 IN-SILICO ANALYSIS OF nsSNPs (COMPUTATIONAL TOOLS)

As genomic variations among people, Single Nucleotide Polymorphisms (SNPs) exist throughout the genome and can be divided into several groups. Among the different kinds of SNPs, a nonsynonymous SNP in the coding region of a gene is important because it alters the amino acid composition; consequently, such alterations can have an impact on protein structure, function, and subcellular localization. There is an exponential expansion of SNPs in databases due to the development of new techniques for the large scale identification of SNPs in the human genome (Wang *et al*., 1998). There are several publically available databases for SNPs, such as dbSNP, GWAS Central, and SwissVar. By release of 135 hosting number of human SNPs reached more than 50million, including 535,660 synonymous and 873,308 non-synonymous SNPs (Luu *et al*., 2012). The major goal of mining this database is to find the relevance of these genetic variations and genotypes; thus providing a basis for therapies for human diseases (Syvanen 2001).

2.9 SNP GENOTYPING: PCR-RFLP

SNP genotyping is performed by many methods, including hybridization, allele-specific 10 polymerase chain reaction (PCR), primer extension, oligonucleotide ligation, direct DNA sequencing, and endonuclease cleavage. Each of these methods has its specific advantages and disadvantages.

If the SNP to be studied involves a restriction enzyme site, Polymerase Chain Reaction - Restriction Fragment Length Polymorphism (PCR-RFLP) can be a genotyping procedure that is easy to set up in any molecular biology laboratory. The PCR-RFLP method allows very rapid, simple, and inexpensive detection of point mutations within the sequences of PCR products. The mutation is discriminated by the specific restriction endonuclease and is identified by gel electrophoresis followed by staining with ethidium bromide. This convenient and simple method is useful in a small basic research study.

PCR-RFLP involves two steps:

1. PCR: Biochemical reactions to form allele-specific products and

2. RFLP: detection procedures to identify the products.

2.10 POLYMERASE CHAIN REACTION

The polymerase chain reaction (PCR) is a biochemical technology in molecular biology to amplify a single or a few copies of a piece of DNA into thousands to millions of copies of a particular DNA sequence. The method relies on thermal cycling which

consisting of cycles of repeated heating and cooling of the reaction for DNA melting and enzymatic replication of the DNA.

There are three major steps in a PCR, which are repeated for 30 or 40 cycles. This is done on an automated thermocycler, which can heat and cool the tubes with the reaction mixture in a very short time.

- Denaturation: In this step, reaction is heated to 94–98 °C for 20–30 seconds. It causes DNA melting of the DNA template by disrupting the hydrogen bonds between complementary bases, yielding single-stranded DNA molecules.
- Annealing: As the temperature cools down to its annealing temperature, primers anneals with single strand DNA i.e. short oligonucleotide primer sequence bind with the complementary region of DNA and forms a stable bond.
- Extension: 72˚C is the ideal working temperature for the Taq polymerase enzyme. The polymerase adds dNTPs from 5' to 3'and reading the template from 3' to 5' side. The initiation of DNA synthesis occurs at 3'-hydroxly end of each primer. The primers are extended by joining the bases complementary to DNA strands using Taq polymerase enzyme.

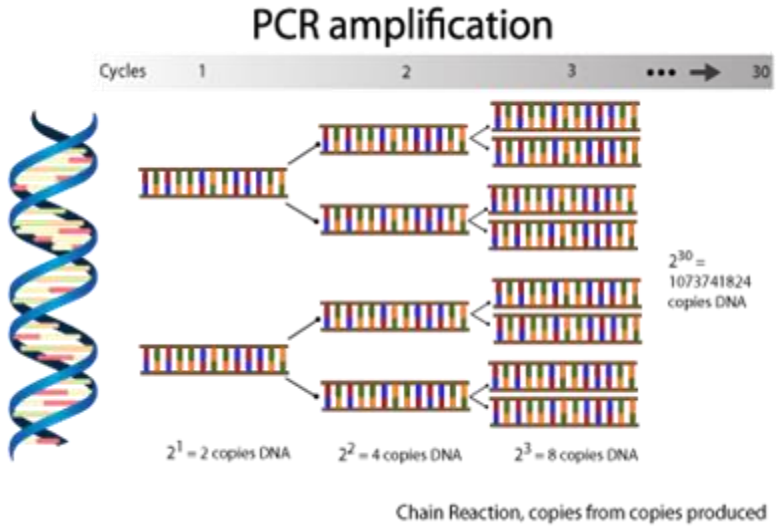

Fig 9: PCR Amplification cycle and major steps (www.gmotesting.com)

2.11 Restriction Fragment Length Polymorphism (RFLP)

RFLP arise because single base pair change can create or destroy the sites recognized by specific restriction enzymes, leading to variation between individual in the length of restriction fragment produced from identical regions of genome. A single base pair change i.e. SNP is readily detectable genetic marker by RFLP because a mutated site is no longer cleaved by the enzyme in question. Two chromosome differ by such a mutation are then distinguishable on the basis of RFLP, which arises because a particular cleavage site is present in only one of the DNA molecule.

CHAPTER 3: OBJECTIVE

This study has been divided into two broad categories, underlying the main objectives of this study.

1. To predict most deleterious non-synonymous SNPs through in-silico analysis of nsSNPs of LXR-α gene.

2.To Optimize PCR for the predicted nsSNPs (rs11545529 and rs61731956).

3. To genotype predicted nsSNPs (rs11545529 and rs61731956) of LXR- α gene by PCR-RFLP in vitiligo patient and control individual belonging to North India.

4.To look for the genetic association, if any, between polymorphism in LXR- α and susceptibility to vitiligo by statistical analysis.

In our study, we would explore the association of LXR-alpha gene polymorphisms (rs11545529 and rs61731956) with vitiligo susceptibility which could be used as informative marker for Vitiligo susceptibility.

CHAPTER 4: MATERIALS AND METHODS

4.A. IN-SILICO ANALYSIS OF nsSNPs OF LXR-α GENE

4.A.1) Data mining

The data on human gene LXR alpha was collected from the Entrez gene on National Center for Biological Information (NCBI) website. The SNP information (protein accession number and SNP ID) of the human LXR alpha gene was retrieved from the NCBI dbSNP.

4.A.2) Sequence homology – based prediction of deleterious nsSNPs by using SIFT.

SIFT (Sorting Intolerant from Tolerant) took a query sequence and used multiple alignment information to predict tolerated and deleterious substitutions for every position entered as the query sequence (Ng and Henikoff, 2003). SIFT server was available at (http://sift.jcvi.org/).

4.A.3) Predicting the functional effects of nsSNPs by PROVEAN

PROVEAN (Protein Variation Effect Analyzer) (http://provean.jcvi.org.). It predicted the functional impact for all classes of protein sequence variations not only single amino acid substitutions but also insertions, deletions, and multiple substitutions on the alignment-based score (Choi *et al*., 2012). The score measured the change in sequence similarity of a query sequence to a protein sequence homolog between without and with an amino acid variation of the query sequence. If the PROVEAN score comes out to be ≤-2.5, the protein variant was predicted to have a "deleterious" effect, while if the PROVEAN score was >-2.5, the variant is predicted to have a "neutral" effect.

4.A.4) 4Predicting protein stability changes using I-Mutant 2.0 and MUpro

4.A.4.1) I-Mutant2.0

I-Mutant2.0 was a Support Vector Machine-based web server for the automatic prediction of protein stability changes introduced by single-site mutations. The predictor evaluated the stability change upon single site mutation starting from the protein sequence. I-Mutant2.0 correctly

predicted whether the protein mutation stabilises or destabilises the protein The protein stability change was predicted from the sequence (I- Mutant2.0-Seq) (http://folding.biofold.org/i-mutant/i-mutant2.0.html). The DDG value (difference in free energy of mutation) was calculated from the unfolding Gibbs free energy value of the variant protein minus the unfolding Gibbs free energy value of the wild type (*kcal/mol*), and scores <0 were predicted by the algorithm to indicate decreased stability, whereas scores >0 were considered to indicate increased stability.

4.A.4.2) MUpro

Mupro (http://mupro.proteomics.ics.uci.edu/mutation_intro.html) was again a support vector machine-based tool for the prediction of protein stability changes upon nonsynonymous SNPs. The value of the energy change was predicted, and a confidence score between -1 and 1 for measuring the confidence of the prediction was calculated. A score <0 meant the variant decreased the protein stability; conversely, a score >0 meant the variant increased the protein stability.

4.A.5) Evolutionary analysis of coding SNPs by PANTHER

The PANTHER (**P**rotein **AN**alysis **TH**rough **E**volutionary **R**elationships) (http://pantherdb.org/tools/csnpScore.do) classified protein according to their family, subfamily, molecular functions, etc. Based on an alignment with evolutionary aspect, the substitution position-specific evolutionary conservation score (subPSEC) was calculated and this estimated the possibility of functional impact on the protein by a particular nsSNP. The subPSEC scores varied from 0 (neutral) to about -10 (most likely to be deleterious) with the scores B-3 being deleterious.

4.A.6) Disease associated SNP prediction by nsSNP analyzer and PhD SNP

nsSNPanalyzer (http://snpanalyzer.uthsc.edu/), was a tool to predict whether a nonsynonymous single nucleotide polymorphism (nsSNP) has a phenotypic effect. nsSNPAnalyzer also provided additional useful information about the SNP to facilitate the interpretation of results, e.g., structural environment and multiple sequence alignment. nsSNPAnalyzer used this information to make predictions.

PhD-SNP (http://snps.biofold.org/phd-snp/phd-snp.html) a predictor based on a single SVM

trained and tested on protein sequence and profile information, classifies mutations into diseases related and neutral polymorphism.

4.A.7) Consensus Classifier for Prediction of Disease-Related Mutations: PredictSNP

The PredictSNP was a consensus classifier combining six best performing prediction methods to provide more accurate and robust alternative to the predictions delivered by individual integrated tools. The predictions from the computational tools were supplemented by experimental annotations from two databases. The web server was freely available to the academic community at http://loschmidt.chemi.muni.cz/predictsnp. The predictions of PredictSNP consensus and individual tools were provided as well as their expected accuracies in the range between 0-100%.

4.A.8) Disease prediction from SuSPect

SuSPect used sequence-, structure- and systems biology-based features to predict the phenotypic effects of missense mutations. It discriminated between disease-causing and neutral variants. SuSPect provided scores predicting whether or not a variant is likely to be associated with disease. It produced a table of scores from 0-100, colour-coded according to predicted deleteriousness (blue=neutral, red=disease-causing).

4.A.9) Prediction of disease related amino acid substitution by MutPred

MutPred (http://mutpred.mutdb.org/) was a web application tool developed to classify an amino acid substitution as disease-associated or neutral in human. In addition, it predicted molecular cause of disease. The tool required a protein sequence, a list of amino acid substitutions, and an email address. It utilized several attributes related to protein structure, function, and evolution (Li, 2009).

4.A.10) Modeling nsSNPs on protein structure and RMSD calculations

4.A.10.1) Predicting secondary structures through PSIPRED

The PSIPERD program (http://bioinf.cs.ucl.ac.uk/psipred/) incorporated PSIPRED, GenTHREADER, and MEMSAT2 methods for protein structure prediction. This prediction method employed two feedforward neural networks, which performed an analysis on the output obtained from PSI-BLAST (Buchan *et al*., 2013).

4.A.10.2) Homology modeling of the native and mutant protein structures using Phyre2

To understand structure–function relationships, 3D structures were required, as point mutations significantly change stability of protein structures. Phyre2 was a suite of tools available on the web to predict and analyze protein structure, function and mutations. Phyre2 (http://www.sbg.bio.ic.ac.uk/phyre2) used the Hidden Markov Method to generate alignments of a submitted protein sequence against proteins with published structures (Kelley and Sternberg, 2009). The resulting alignments were then used to produce homology based models of the query sequence to predict its three-dimensional structure.

4.A.10.3) Calculation of the RMSD values

TM-align (http://zhanglab.ccmb.med.umich.edu/TM-align/) was an algorithm to check for sequence-order independent protein structure comparisons. For two protein structures of unknown equivalence, TM-align first generated optimized residue-to-residue alignment based on structural similarity using dynamic programming tool. An optimal superposition of the two structures, as well as the TM-score value which scales the structural similarity, were returned. TM-score had the value in range (0,1], where 1 indicated a perfect match between two structures. Additionally, it also produced the root-mean-square deviation (RMSD) which was the measure of the average distance between the atoms (usually the backbone atoms) of superimposed proteins.

4.A.10.4) MUSTER

MUSTER was a MUlti-Source ThreadER program, which considered six different sources: (1) sequence-derived profiles; (2) secondary structures; (3) structured-derived profiles; (4) solvent accessibility; (5) torsion angles (psi and phi angles); (6) hydrophobic scoring matrix. The optimized threading was found by global dynamic programming. MUSTER provides the Z-score and complete full length models by using MODELLER v8.2. If the calculated Z-score was greater than 7.5, the corresponding template was considered good otherwise designated as bad (Wu and Zhang, 2008).

4.A.10.5) Energy Minimisation

Total energy of native and mutant structures was calculated using software Discovery Studio 3.5 Client.

4.B. EXPERIMENTAL PROCEDURES

Study population

The study group comprised of total 78 vitiligo patients (44 male/ 34 female). A total of 120 healthy individuals with no history of vitiligo or apparent autoimmune disease were included as control; they matched to patients with regard to age, sex and geographical distribution. Written consent was signed by all the individuals before drawing the blood sample, in addition to imparting knowledge about the project to all.

4.B.1) Sampling

2ml venous blood was collected from the patients and healthy subjects in Na_2EDTA coated tubes. Blood sample are stored at -20˚C till further use.

4.B.2) Isolation of Genomic DNA from Whole Blood sample (Miller *et.al.*, 1988)

- 400µl blood sample was pippetted in a 2ml eppendorf. To this RBC lysis buffer was added (three times the volume of blood sample) and was kept for incubation on a rocker at room temperature until RBCs completely lysed. (Appendix 2.6)
- The solution was centrifuged at 13,000 rpm for 1 min to obtain a creamish white WBC pellet.
- The supernatant was discarded and the WBC pellet was thoroughly suspended in 400 µl TE buffer (pH 8.0) using a vortexing machine. (Appendix 2.7)
- 22 µl of 10% SDS solution was added to the suspended pellet solution and the mixture was incubated at 56o C for 30 min on a dry bath. (Appendix 2.5)
- Subsequently, 160 µl of 7.5 M ammonium acetate was added to the solution and was mixed vigorously for about 1 min per sample on vortexer. The mixture was
- centrifuged at 13,000 rpm at RT for 15 mins, thereby resulting in separation of the precipitated proteins as pellet.

- The clear supernatant was transferred to a fresh sterile micro-centrifuge. To this chilled absolute ethyl alcohol was added (twice the volume of clear supernatant). the tube was gently rocked a couple of times to allow the precipitation of genomic DNA.
- The genomic DNA precipitate was centrifuged at 13,000 rpm for 10 min to pellet at the bottom of the tube. The latter were subsequently washed in 150 µl of 70% ethanol and air dried at RT for about 10-15 mins.
- The dried pellet was dissolved in 40 µl TE buffer (pH 7.3) by incubating at 65oC for 10 mins. The dissolved DNA was finally stored at 20oC till further use.(Appendix 2.8)
- The DNA quantification was done using Nano Drop plus Spectrophotometer (GE Healthcare, US). The concentration of DNA was read by measuring the absorbance of a sample at A260 on a spectrophotometer.

4.B.3) Primer Designing

Designing oligonucleotide primers is a crucial step for successful molecular biology experiments that require the use of PCR. PCR involves cycles of three steps: denaturation, annealing, and extension. The goals of primer design include good primer specificity, high annealing efficiency, appropriate melting temperature, proper GC content, and the prevention of primer hairpins or primer dimers.

4.B.3.1) Protocol for designing primer:

a) NCBI (National Center for Biotechnology Information) webpage was opened.

b) Primer BLAST option was selected and the nucleotide sequence was entered into the query box.

c) 'Get Primers' option was selected.

d) The primer pair (forward and reverse) from the list of the primers was generated.

4.B.3.2) Protocol for primer tailing: Primer tailing

a) A nucleotide base in the reverse primer (or forward primer) was changed on order to generate the restriction site.

b) A polynucleotide tail of about 40 nucleotides was added onto the 5' end of the primer.

Table 5: Primers for selected nsSNPs

nsSNPs ⟹	**rs11545529**	**rs61731956**
Forward Primer	AGTCCTAGCTAGAGCCCACACAGAC	TGACCTATAGACCGGCCCAA
Reverse Primer	CCCAAAAAAAAAAACCCCCCCCCCAAAAAAAAAAGGGGCATCCTGGCTTCCTCTCTGAGGC	GGCCATACCACAGAGTGACA
Tm (˚ C)	66.75	57.25
Amplicon size	303bp	798bp

4.B.3.3) Reconstitution of Primers (Lyophilized)

For 100µM, following amount of distilled water (d.w.) was added.

Table 6: Amount of distilled water added to the primers for reconstitution

Primers	**d.w. (µl)**
rs956F	262
rs956R	278
rs529F	295
rs529R	259

4.B.4) PCR Optimization

4.B.4.1) Gradient PCR

Gradient PCR was performed for both set of primers to identify the best annealing temperature for the successive amplification of the specific product.

4.B.4.2) PCR: Biochemical reaction to form allele specific product

PCR technology was used for the amplification of the desired LXR-alpha gene segment. PCR amplification of the genomic DNA isolated from blood sample was carried out using primers (Table 4) specific for the LXR-Alpha gene sequence which were made using software PRIMER3. Polymerase chain reaction for the LXR-alpha gene amplification was performed using the following protocol:

- 12.5µl reaction mixture was prepared as per the composition given in the Table 6. Samples mixture was kept into the Thermocycler (Thermo scientific thermocycler) for amplification and parameters as given in Table were set.

Table 7: Reagent Mixture Composition used in the PCR for DNA Amplification

Reaction component	**Per reaction volume (µl)**
Master mix	6
DNA template	1
Forward Primer	0.25
Reverse Primer	0.25
Nuclease free water	5
Total	**12.5**

Table 8: PCR Cycling conditions for the amplification of Genomic DNA

nsSNP: rs11545529

Step	Temperature (˚C)	Time	Cycles
Initial Denaturation	94	2 min	
Final Denaturation	94	30 sec	35 cycles
Annealing	70	30 sec	
Extension	72	30 sec	
Final Extension	72	5 min	
Final Hold	4	infinite	

nsSNP: rs61731956

Step	Temperature (˚C)	Time	Cycles
Initial Denaturation	94	1 min	
Final Denaturation	94	30 sec	35 cycles
Annealing	56	30 sec	
Extension	72	30 sec	
Final Extension	72	5 min	
Final Hold	4	infinite	

4.B.5) Genotyping: PCR – RFLP

Restriction Fragment Length Polymorphism (RFLP) was used to identify the allele specific product.

Amplified product was digested with the restriction enzyme to identify the genotype present in a particular individual. PCR product of rs11545529 and rs61731956 were digested with PstI and BspEI respectively. Reaction condition of RFLP for both the nsSNPs are mentioned in Table 8.

Table 9: Reaction Condition of RFLP Genotyping Method

Reaction Component	*Reaction volume (µl)*	
	rs11545529	rs61731956
	PstI	BspEI
	5′CTGCA|G 3′ 3′G|ACGTC 5′	5′T|CCGGA 3′ 3′AGGCC|T 5′
Enzyme	0.13	0.2
Buffer	1.5	2
Water	3.37	2.8
DNA	10	10
Total	15	15

Analysis of Digested PCR Product:

Agarose gel electrophoresis was done to visualize the digested band pattern. Digested Band pattern for different genotype is as shown in fig and Table 10.

RFLP digested product were analyzed on 3% w/v (rs11545529) and 2% w/v (rs61731956) agarose gel containing Ethidium Bromide (0.5mg/ml). A NEB 50 bp (rs11545529) and 100 bp (rs61731956) marker was used as ladder. 15 µl of amplified product was loaded into the wells along with ladder into the separate well. The gel was then run for 40-50 min at 100Volts in 1X-TAE buffer. Bands were visualized using U.V. transilluminator.

Table 10: Digested band pattern of SNP rs11039155 and rs2279238

rs11545529		**rs61731956**	
Genotype	Band size (bp)	Genotype	Band size (bp)
GG	303	AA	798
AG	236+67+303	AG	343+455+798
AA	236+67	GG	343+455

4.B.6) Statistical Analysis

Statistical tools were applied to assess the association of LXR-alpha gene polymorphism with vitiligo susceptibility.

The significant differences in genotype and allele frequencies between patients and controls were analyzed by the Fisher exact test (http://www.quantpsy.org/fisher/fisher.htm). A chi-squared test was used to determine whether observed control genotype frequencies conformed to Hardy-Weinberg equilibrium (HWE) expectation using online HWE calculator (http://www.had2know.com/academics/hardy-weinberg-equilibrium-calculator-2 alleles.html). Observed frequency considered to be in disequilibrium if $p < 0.05$. Odds ratios and 95% confidence intervals were calculated to assess the risk associated with variant allele. Odd Ratio was calculated using MedCalc software (https://www.medcalc.org/calc/odds_ratio.php). The significance of the odd ratio was determined by Z test ($p<0.05$ was considered statistically significant).

CHAPTER 5: OBSERVATIONS AND RESULTS

5.A. IN-SILICO ANALYSIS

5.A.1) SNP analysis

In recent years, nsSNPs have emerged as diagnostic markers, since they are closely related with various diseases and their development. By examining LXR-alpha gene using dbSNP, a total of 6 non synonymous SNPs were found.

5.A.2) Deleterious nsSNPs from SIFT and PROVEAN programs

Protein sequence with mutational position and amino acid residue variants associated to 206 missense nsSNPs were submitted as input in the SIFT server, and the results are shown in Table 11. Among the total nsSNPs analysed, 3 nsSNPs were identified to be deleterious with a tolerance index score ≤0.05. Two nsSNP (rs61731956 and rs41275182) showed a highly deleterious tolerance index score of 0.00. The remaining nsSNPs (rs2167079, rs41481445 and rs78765998) were found to be tolerated with tolerance index scores of ≥0.05.

The results obtained from the sequence based predictor PROVEAN sorted out the variants that were predicted to be “Deleterious” when the final score is below the threshold (default is −2.5), and that were predicted to be “Neutral” when the score was above the threshold. It was observed that out of 6 nsSNPs, only one nsSNP was predicted as “Deleterious” and had a PROVEAN score of below −2.5.

Table 11: Prediction of the effect of nsSNPs of HSD3B2 using SIFT and PROVEAN server.

S.No.	dbSNP ID	Allele	Residue change	SIFT prediction(score)	PROVEAN prediction(score)
1	rs41275182	A/G/T	R10W	**Damaging**(0.00)	-
2	rs2167079	A/G	R29Q	Tolerated(1)	-
3	rs11545529	A/G	I39V	**Damaging**(0.02)	Neutral(0.112)
4	rs41481445	C/G/T	G52V	Tolerated(0.24)	Neutral(-1.409)
5	rs78765998	A/T	H339Q	Tolerated (0.18)	Neutral(0.599)
6	rs61731956	A/G	R355Q	**Damaging** (0.00)	**Deleterious**(-3.786)

6.A.3) **Prediction of change in stability due to mutation**

The I-Mutant 2.0 server calculated the DDG values, tested with the data extracted from ProTherm, the most comprehensive available database of thermodynamic experimental data of free energy changes of protein stability due to mutation. It was observed that there was a large decrease of stability for variants R10W, I29V, H339Q and R355Q. Other mutants exhibited increased stability. These results are summarized in Table 12.

MuPro Predicted the sign of energy change using Support Vector Machines indicating the effects of mutation on protein stability. A confidence score between -1 and 1 was used to measure the confidence of the prediction. A score less than 0 meant the mutation decreases the protein stability. The smaller the score, the more confident the prediction was. Three variants (I39V, H339Q and R355Q) out of 4 were predicted to decrease the stability with scores less than 0.

Table 12: Stability prediction of LXR-alpha protein upon amino acid substitution by IMutant and Mupro. Stability was predicted as DDG Value=DG (NewProtein) − DG (WildType) in Kcal/mol.

S.No	dbSNP ID	I-Mutant 2.0 prediction (DDG)	MuPro prediction (Score)
1	rs41275182	**Decrease** (-1.73)	-
2	rs2167079	Increase (0.64)	-
3	rs11545529	**Decrease** (-0.92)	**Decrease** (-1)
4	rs41481445	Increase (0.04)	Increase (0.00782163)
5	rs78765998	**Decrease** (-0.35)	**Decrease**(-0.35495772)
6	rs61731956	**Decrease** (-1.17)	**Decrease** (-0.35335799)

6.A.4) **Disease associated nsSNP prediction by nsSNPAnalyzer, PANTHER and Phd-SNP**

The results obtained from nsSNPAnalyzer and PhD-SNP and, from PANTHER are summarized in the table 13 and table 14 respectively. It was observed that only one nsSNP (rs61731956) out of 6 was predicted to be 'disease associated'.

On the other hand, PANTHER used the family HMMs to rank missense single nucleotide polymorphisms (SNPs), on a database-wide scale, according to their likelihood of affecting protein function. The substitution PEC score is simply the difference between the aaPSEC scores for the two alleles. When subPSEC = 0, the substitution is interpreted as functionally neutral, whereas more negative values of subPSEC predict more deleterious substitutions. Hence, it reported two variants (H339Q and R355Q) to be disease associated, with negative subPSEC scores respectively.

Table 13: Results obtained from disease-associated nsSNPs prediction by PANTHER and PhD-SNP

S.No.	dbSNP ID	Allele	Residue change	PANTHER subPSEC	Pdeleterios	PhD-SNP Effect	RI
1	rs41275182	A/G/T	R10W	-	-	Neutral	8
2	rs2167079	A/G	R29Q	-	-	Neutral	6
3	rs11545529	A/G	I39V	-	-	Neutral	7
4	rs41481445	C/G/T	G52V	-	-	Neutral	5
5	rs78765998	A/T	H339Q	-0.62	0.08	Neutral	6
6	rs61731956	A/G	R355Q	-4.96	0.88	**Disease**	6

Table 14: Output for nsSNPAnalyzer

SNP	Amino acid variant	Phenotype	Environment	Area buried	FracPolar	Secondary structure
rs61731956	R355Q	**Disease**	P2H	0.43	0.9	H

6.A.5) **Concordance analysis of predicted results using in-silico tools**

The accuracy of deleterious nsSNPs predicted can be increased by combining different computational methods. For the results we could infer that, one SNP (rs61731956) out of 6 was predicted to be deleterious with 82%, highest score reported by PhD-SNP, followed by Polyphen 2 and SNAP at 81% (Table 15).

Table 15: List of "possible deleterious ns-SNPs" by combined prediction

Mutation	Predict SNP	MAPP	PhD-SNP	Polyphen-1	Polyphen-2	SIFT	SNAP	nsSNPAnalyzer	PANTHER
I39V	83.00%	72.00%	78.00%	67.00%	87.00%	73.00%	71.00%	-	-
G52V	83.00%	73.00%	88.00%	67.00%	72.00%	63.00%	68.00%	-	71.00%
H339Q	83.00%	80.00%	72.00%	67.00%	74.00%	87.00%	61.00%	-	71.00%
R355Q	75.00%	46.00%	82.00%	67.00%	81.00%	79.00%	81.00%	65.00%	-

Neutral	Deleterious	XX % confidence

6.A.6) **Prediction of disease associated nsSNPs from SuSPect**

SuSPect predicted one variant R355Q to be disease associated with reported score of 67, as shown in the figure below (Fig 10).

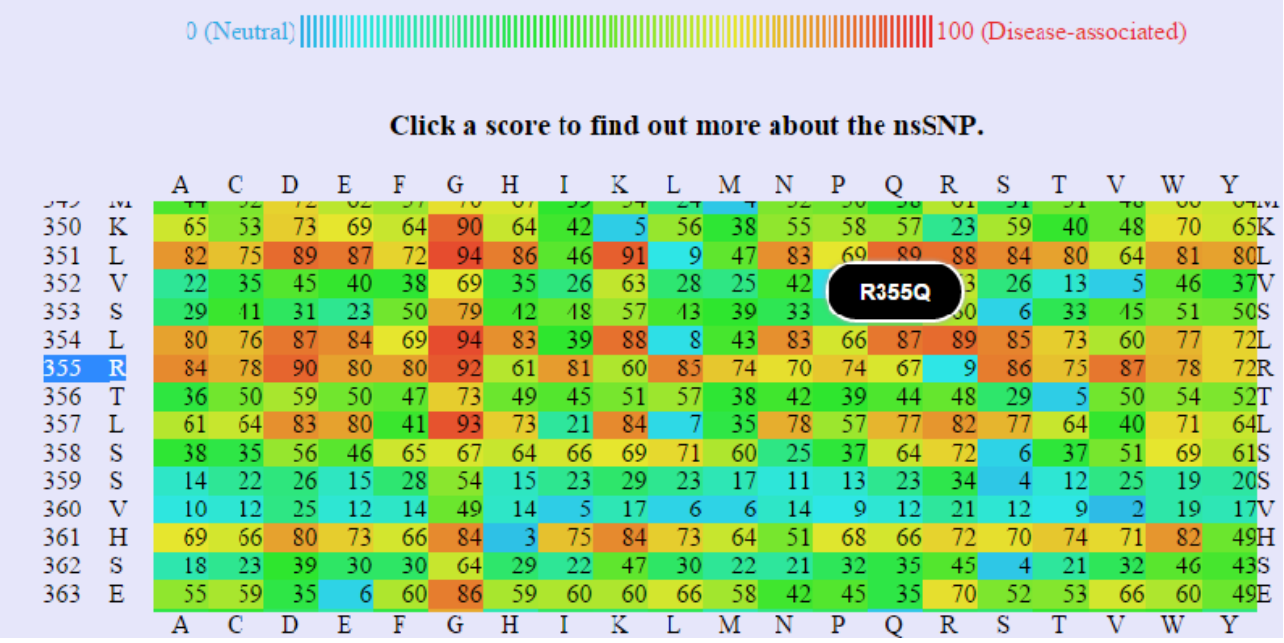

Figure 10: Image showing the output of SuSPect, depicting the score of variant R355Q, predicted to be associated with disease.

6.A.7) **Disease related amino acid substitution prediction by MutPred**

Table 16 summarized the result obtained from MutPred server. Probability of deleterious mutation score for I39V, G52V, H339Q and R355Q was 0.221, 0.108, 0.429, and 0.850 respectively. This implied that some nsSNPs may account for potential structural and functional alterations of LXR-alpha.

Table 16: Analysis of the effect of nsSNPs in LXR-alpha structure, function, and evolution by MutPred server.

Mutation	Probability of deleterious mutations	Molecular mechanism disrupted (Confident hypothesis)	Top 5 features
I39V	0.22	-	Gain of sheet (P = 0.0477) Gain of phosphorylation at S36 (P = 0.2193) Loss of stability (P = 0.2233) Loss of loop (P = 0.2237) Gain of methylation at R41 (P = 0.2392)
G52V	0.11	-	Loss of glycosylation at S49 (P = 0.0715) Loss of phosphorylation at S49 (P = 0.166) Loss of catalytic residue at T53 (P = 0.2379) Gain of MoRF binding (P = 0.3584) Gain of solvent accessibility (P = 0.4946)
H339Q	0.43	-	Gain of solvent accessibility (P = 0.0216) Gain of relative solvent accessibility (P = 0.0275) Gain of MoRF binding (P =

			0.1288) Loss of catalytic residue at D340 (P = 0.1859) Loss of disorder (P = 0.3257)
R355Q	**0.85**	Loss of MoRF binding (P=0.0269)	Loss of MoRF binding (P = 0.0269) Loss of phosphorylation at S358 (P = 0.0703) Loss of methylation at R355 (P = 0.0732) Gain of ubiquitination at K350 (P = 0.1063) Gain of disorder (P = 0.1573)

6.A.8) **Secondary structure prediction by PSIPRED**

The results revealed a clear distribution of alpha helix, beta sheet and coil (Fig 11). Coils dominated among secondary structure elements (61.24%) followed by alpha helix (37.72%) and beta sheet (2.06%).

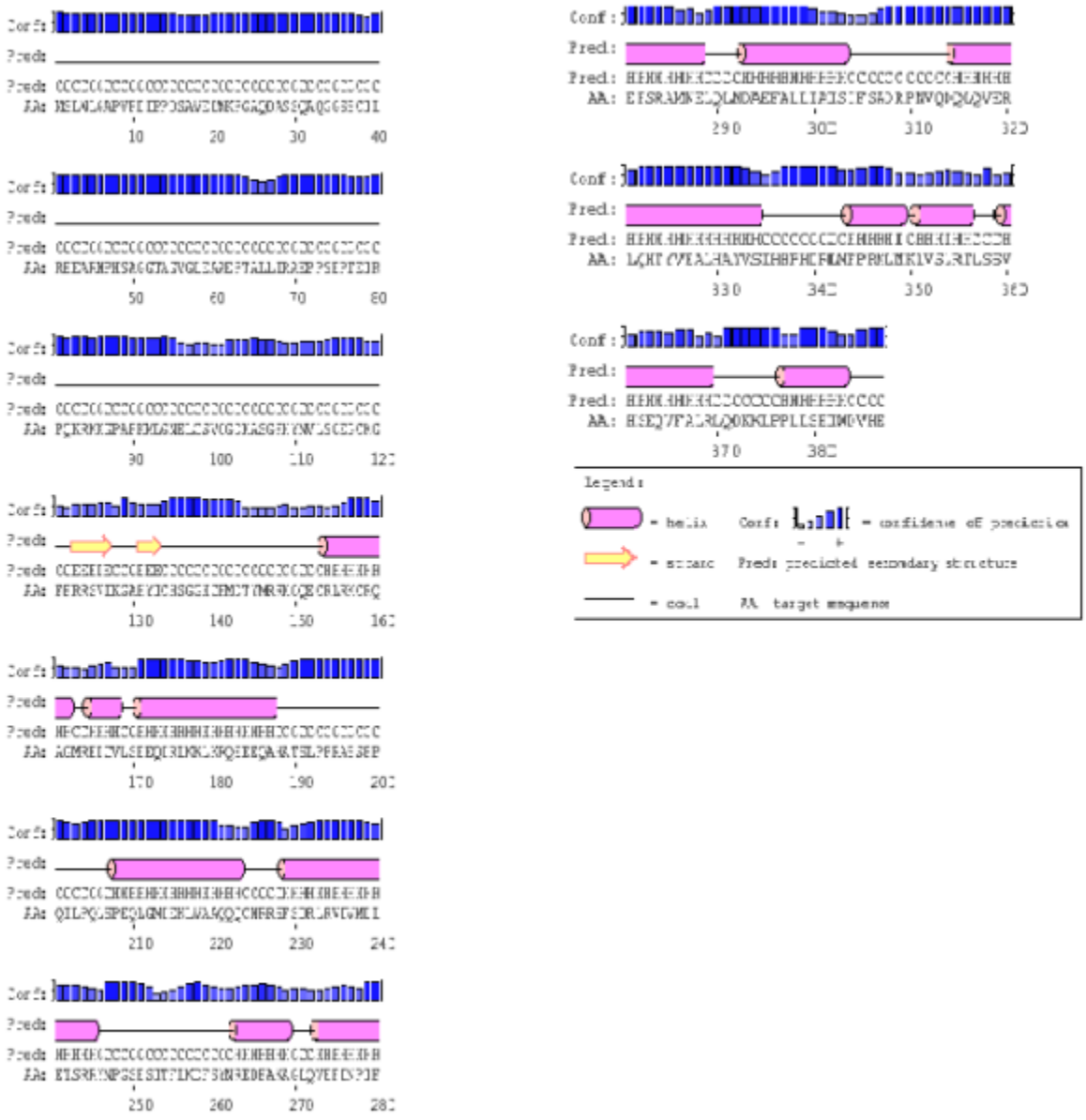

Figure 11: Prediction of secondary structure of LXR-alpha by PSIPRED server.

6.A.9) **Homology modeling of LXR-alpha by Phyre2**

The ability of the protein to interact with other molecules or to have different functions depends upon its tertiary structure Therefore, analysis of damaged coding nsSNPs at the structural level is necessary to understand the activity of the protein. Phyre2 uses the Hidden Markov Method to generate alignments of a submitted protein sequence against proteins with published structures. Figure 12 showed the predicted structure of the native protein of LXR-alpha gene.

The amino acid substitutions which have potential impact on LXR-alpha structure–function were shown in the Fig. 13 and Fig.14

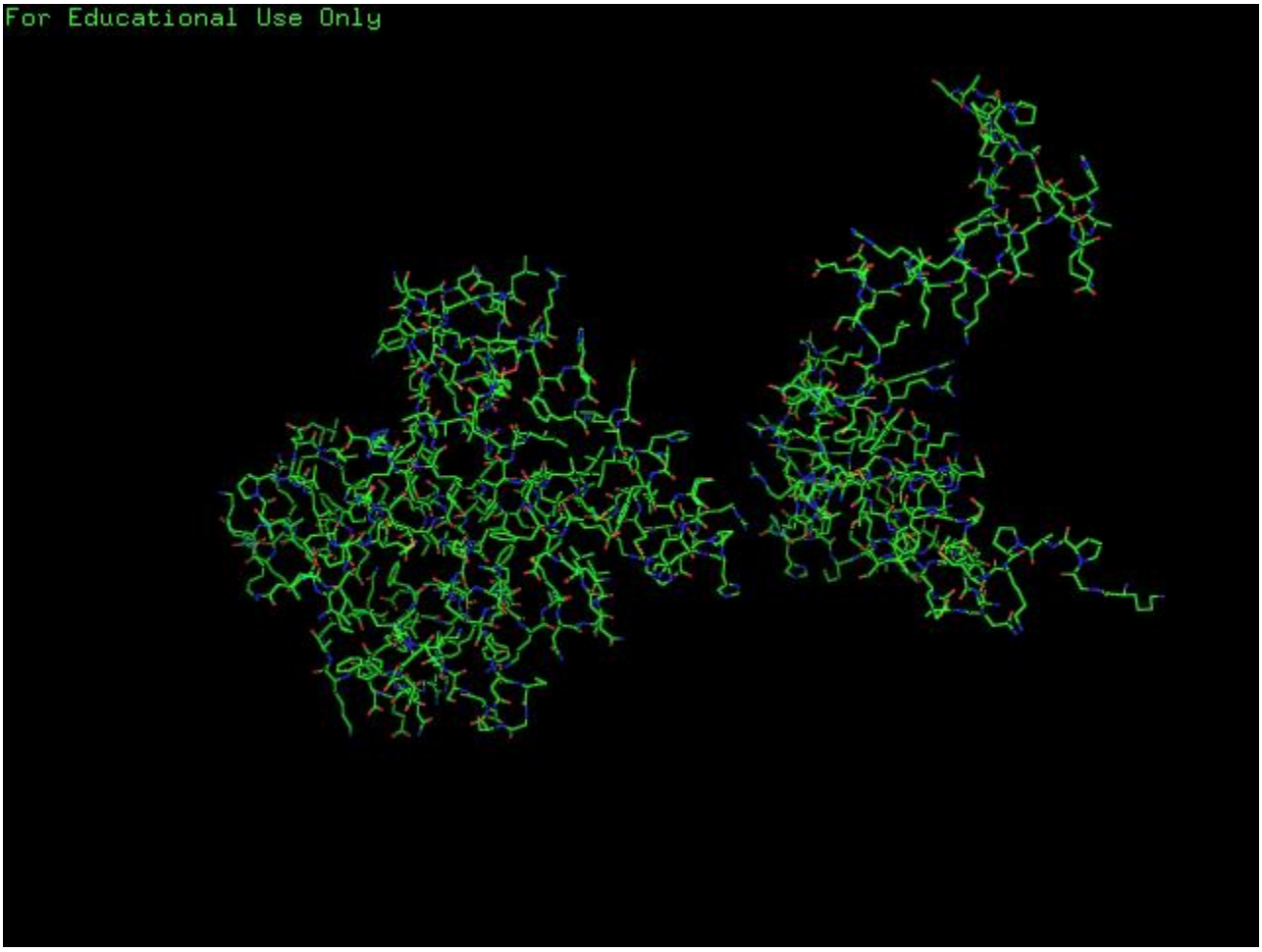

Figure12: The visual image of the structure of LXR-alpha generated in PyMol.

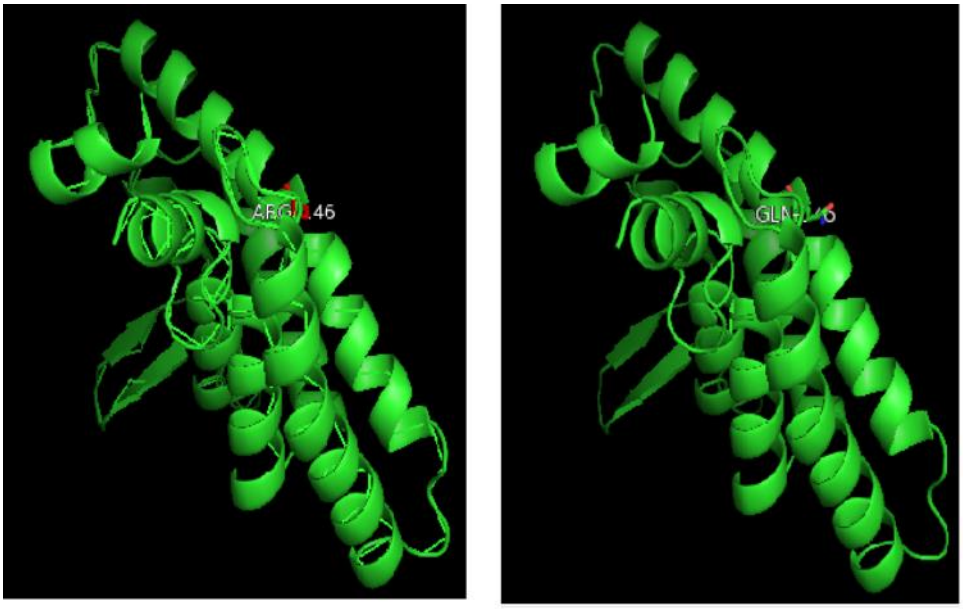

Figure 13: Cartoon representation of predicted models of a) native and b) mutant (R355Q) after structure refinement by PyMol

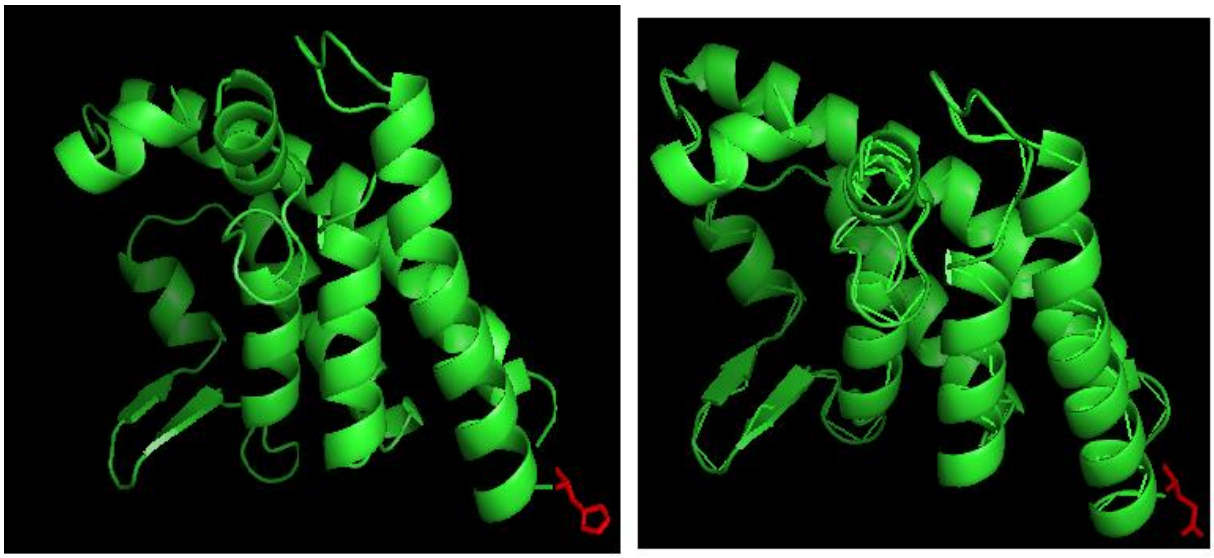

Figure 14: Cartoon representation of predicted models of a) native and b) mutant (H339Q) after structure refinement by PyMol

6.A.10) **Model validation for LXR-alpha by MUSTER**

If Z-score was found to be greater than 7.5, the corresponding template was considered good otherwise designated as bad. It was found (Table 17) that for all the alignments of LXR-alpha score was >7.5, which indicated that all the templates were considered as good type

Table 17: Z score value of different templates analyzed by MUSTER

Rank	Template	Align_Length	Coverage	Z-score	Seq_id	Type
1	3dzyA	289	0.75	13.76	0.27	Good
2	4nqaB	300	0.78	11.68	0.65	Good
3	3e00D	289	0.75	10.92	0.28	Good
4	2qw4A	223	0.58	7.84	0.23	Good
5	1pq6B	235	0.61	7.73	0.52	Good
6	1xdkB	230	0.59	7.7	0.22	Good
7	1pduA	220	0.57	7.62	0.2	Good
8	2e2rA	217	0.56	7.6	0.19	Good
9	2h79A	253	0.65	7.52	0.19	Good
10	1hg4A	228	0.59	7.5	0.18	Good

6.A.11**) Calculation of RMSD values by Tm-Align**

To examine the extent to which mutation effects protein structure, RMSD values were determined for native and mutant protein structure. We calculated the RMSD for all the atoms from the initial structure, which were considered as a central criterion to measure the convergence of the protein system concerned. Throughout the analysis, mutant models H339Q (rs78765998) and R355Q (rs61731956) showed maximum

deviation with RMSD values 1.20. It led to the conclusion that the mutations could affect the dynamic behaviour of mutant protein, thus providing a suitable basis for further analyses.

6.A.12) **Energy minimisation of models by Discovery studio 3.5 client**

Discovery Studio was a comprehensive software suite for analyzing and modeling molecular structures, sequences, and other data of relevance to life science researchers. The product included functionality for viewing and editing data along with tools for performing basic data analysis. The pdb structures of the models generated through Phyre2 were submitted as input to this software and the energy minimisation values (Table 18) were calculated.

Table 18: Total energy of native and mutant structures after energy minimization.

S.No	Model	Total Energy (kcal/mol)
1	Native protein	-16894.77
2	Mutant I39V	-16678.86
3	Mutant G52V	-16848.87
4	Mutant H339Q	-16910.22
5	Mutant R355Q	-16712.61

- Sequence analysis results showed that mutations I39V (rs11545529) and R355Q (rs61731956) had lowest protein stability.
- Structural analysis results showed that the amino acid residue substitutions which had the greatest impact on the stability of the LXR-α protein were mutations H339Q (rs78765998) and R355Q (rs61731956).

B. EXPERIMENTAL RESULTS

Clinical and demographic characteristics of vitiligo patients are shown in Table 19. The sex ratio was almost equal 44% female (34 out of 78) and 56% males (44 out of 78). The range age of patient and control were 18-65 and 25-28 respectively. The average age at onset of disease was varying widely. The majority of patients (88%) had less than 25% body coverage of the depigmented patches. 4% reported the family history of vitiligo. The genotype and allele frequencies of LXR-alpha polymorphisms (rs11545529 and rs61731956) in 78 vitiligo patients and 120 controls are summarized in Table 20.

78 vitiligo patient and 120 control subject were genotyped for **+10906 A*>G** and **+19640 G*>A** in LXR-α gene. The genotype distribution for both the SNP showed no deviation from Hardy-Weinberg equilibrium in control population ($p>0.05$). Genotyping of the SNPs in the LXR-α gene revealed that the variant G allele of rs11545529 was found in 19% of controls and 21% of cases; the variant A allele of rs61731956 was found in 5% of controls and 7% of cases. The allelic frequencies of these two SNPs between vitiligo and control were, rs11545529: $p=0.5197$; rs61731956: $p=0.5318$, which suggested no association of minor allele of both the SNP with the vitiligo. **+10906** G and **+10906** A alleles were found to have no relation to the risk of vitiligo. (**rs11545529**: odds ratio (OR) =0.8462; 95% confidence interval (CI) =0.5090-1.4068; **rs61731956:** OR= 0.7568; 95% CI =0.31-1.81).

Table 19: Clinical and Demographic Characteristics of Vitiligo cases and Control group characteristics

Characteristics	**Vitiligo (N=78)**	**Control (N=120)**
Sex (n/N[%])		
Female	34/78 [44]	56/120 [47]
Male	44/78 [56]	64/120 [53]
Age	18 - 65	25 ± 4
Age at onset		
Changing size of depigmented patches (n/N [%])	24/78 [31]	
Body Coverage of depigmented patches (%)		
1-25	88	
26-50	7	
51-75	3	
76-100	2	
Reported Family history of vitiligo (n/N [%])	3/78 [4]	
White patches at Injury site (n/N [%])	0	

Table 20: Allele and Genotype distribution of the Liver X Receptor-alpha polymorphism in Vitiligo cases (N=78) and control (N=120)

Genotype/Allele	Vitiligo (n/N[%])	Control (n/N[%])	Odds ratio (OR)	95% CI	p-Value
rs11545529					
AA	53/78[68]	78/120[65]			
AG	21/78[27]	33/120[27.5]	0.8462	0.5090-1.4068	0.5197
GG	04/78[05]	09/120[7.5]			
G	29/156[19]	51/240[[21]			
A	127/156[81]	189/240[79]			
rs61731956					
GG	72/78[92]	108/120[90]			
GA	04/78[5]	08/120[7]	0.7568	0.31-1.81	0.5318
AA	02/78[3]	04/120[3]			
A	8/156[5]	16/240[7]			
G	148/156[95]	224/240[93]7			

➢ PCR GRADIENT GEL IMAGES

a) rs11545529

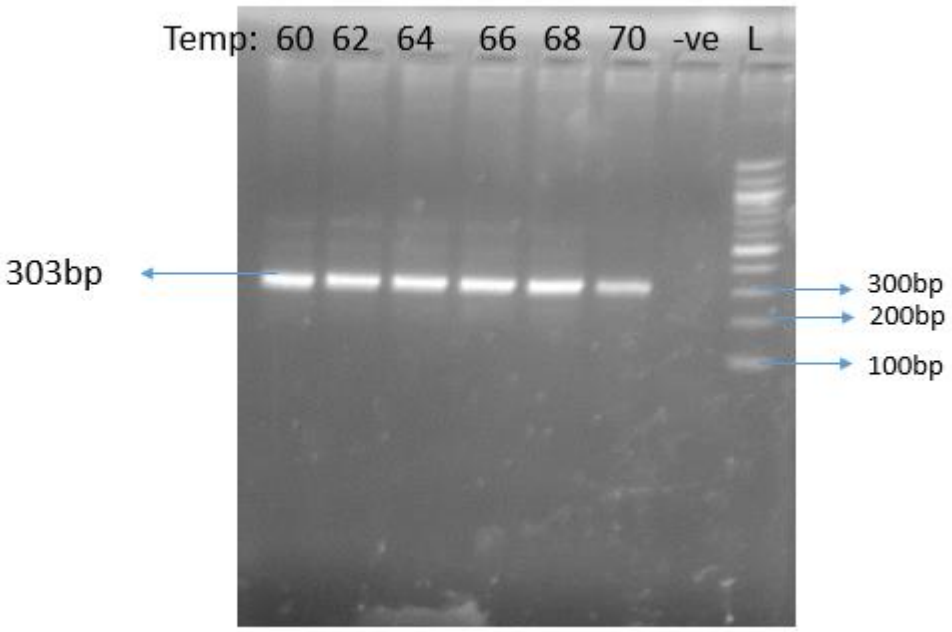

Fig 15 a) Agarose gel electrophoresis (2% agarose w/v) illustrating amplification of single DNA sample (NO.4) at different annealing temperatures 60˚C -70˚C. (Expected band size = 303bp)

Lane1: DNA Sample at temperature 60˚C; **Lane2**: DNA Sample at temperature 62˚C; **Lane 3**: DNA Sample at temperature 64 ˚C; **Lane 4**: DNA Sample at temperature 66˚ C; **Lane 5**: DNA sample at temperature 68˚C; **Lane 6**: DNA sample at temperature 70˚C. **Lane 7**: Negative control; **Lane 8**: 100 bp Ladder.

b) rs61731956

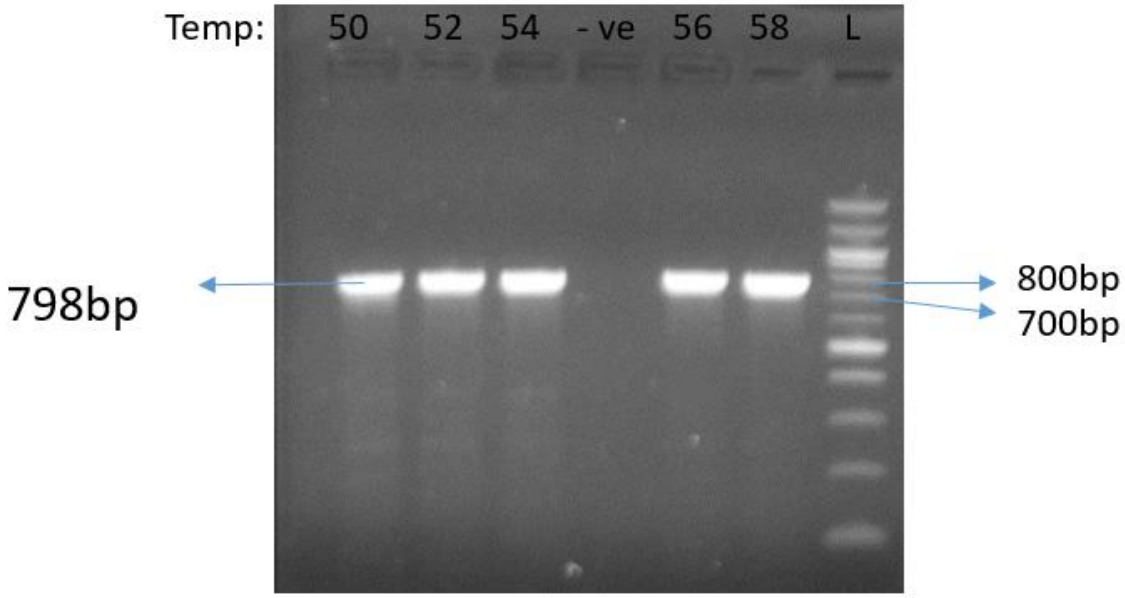

Fig 15 b) Agarose gel electrophoresis (1% agarose w/v) illustrating amplification of single DNA sample (NO.4) at different annealing temperatures 50˚C -58˚C. (Expected band size = 798bp)

Lane1: DNA Sample at temperature 50˚C; **Lane2**: DNA Sample at temperature 52˚C; **Lane 3**: DNA Sample at temperature 54 ˚C; **Lane 4**: Negative control; **Lane 5**: DNA sample at temperature 56˚C; **Lane 6**: DNA sample at temperature 58˚C. **Lane 7**: 100 bp Ladder.

➢ PCR AMPLIFIED PRODUCT

a) rs11545529

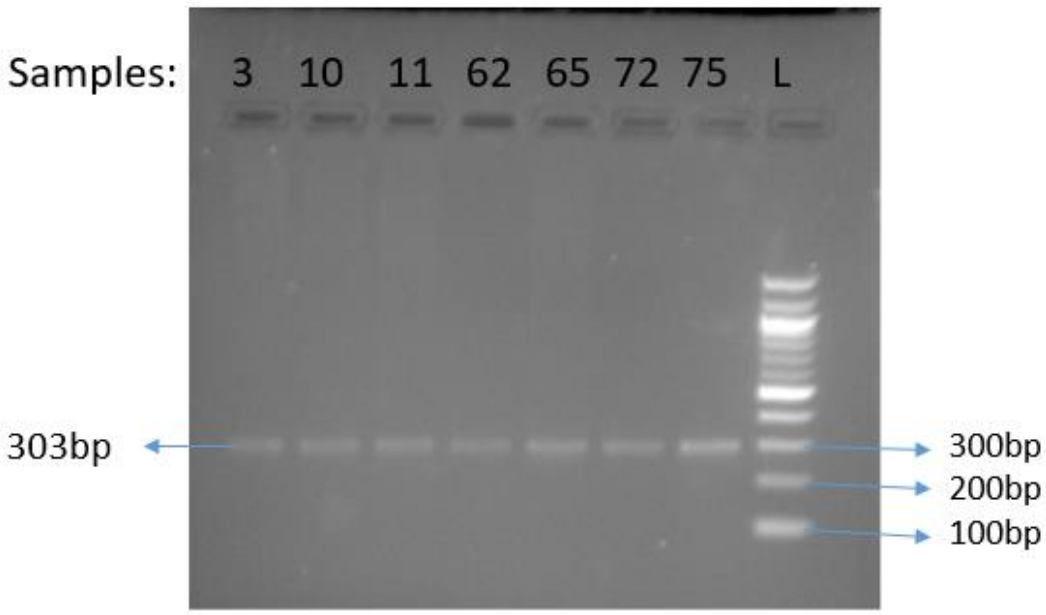

Fig 16 a) Agarose gel electrophoresis (2% agarose w/v) illustrating amplification of 7 DNA samples at single annealing temperatures 70˚C. (Expected band size = 303bp)

Lane1: DNA Sample 3; **Lane2**: DNA Sample 10; **Lane 3**: DNA Sample11; **Lane 4**: DNA sample 62; **Lane 5**: DNA sample 65; **Lane 6**: DNA sample 72; **Lane 7**: DNA sample 75; **Lane 8**: 100 bp Ladder.

b) rs61731956

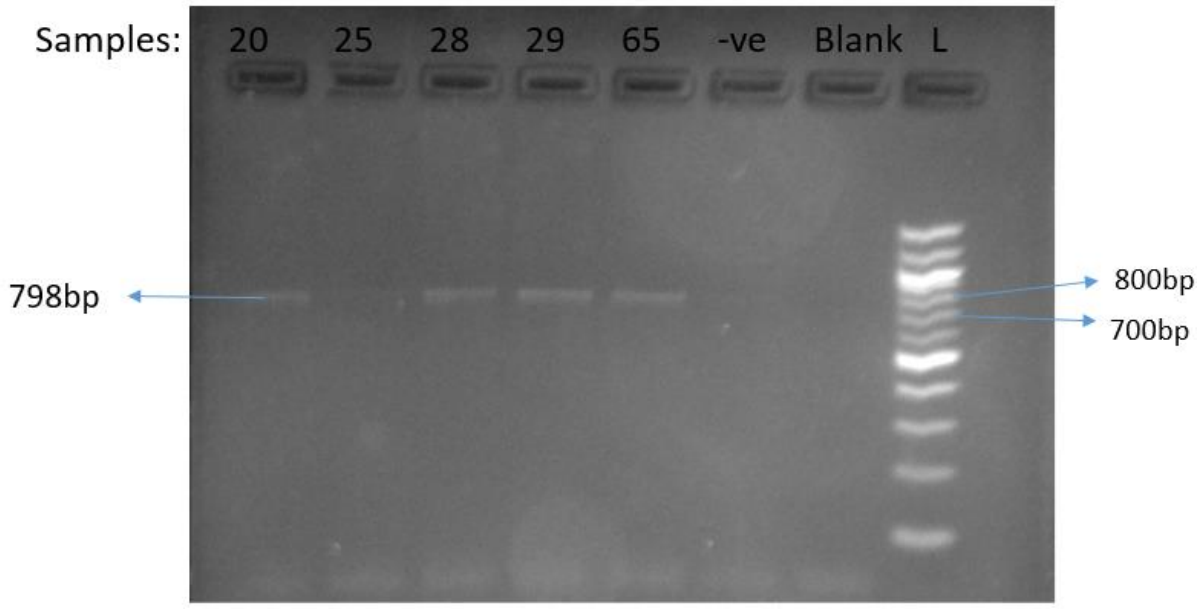

Fig 16 b) Agarose gel electrophoresis (1% agarose w/v) illustrating amplification of 5 DNA samples at single annealing temperatures 56˚C. (Expected band size = 798bp)

Lane1: DNA Sample 20; **Lane2**: DNA Sample 25; **Lane 3**: DNA Sample28; **Lane 4**: DNA sample 29; **Lane 5**: DNA sample 65; **Lane 6**: Negative control; **Lane 7**: blank; **Lane 8**: 100 bp Ladder.

➢ RESTRICTION DIGESTION GEL IMAGE

a) rs11545529

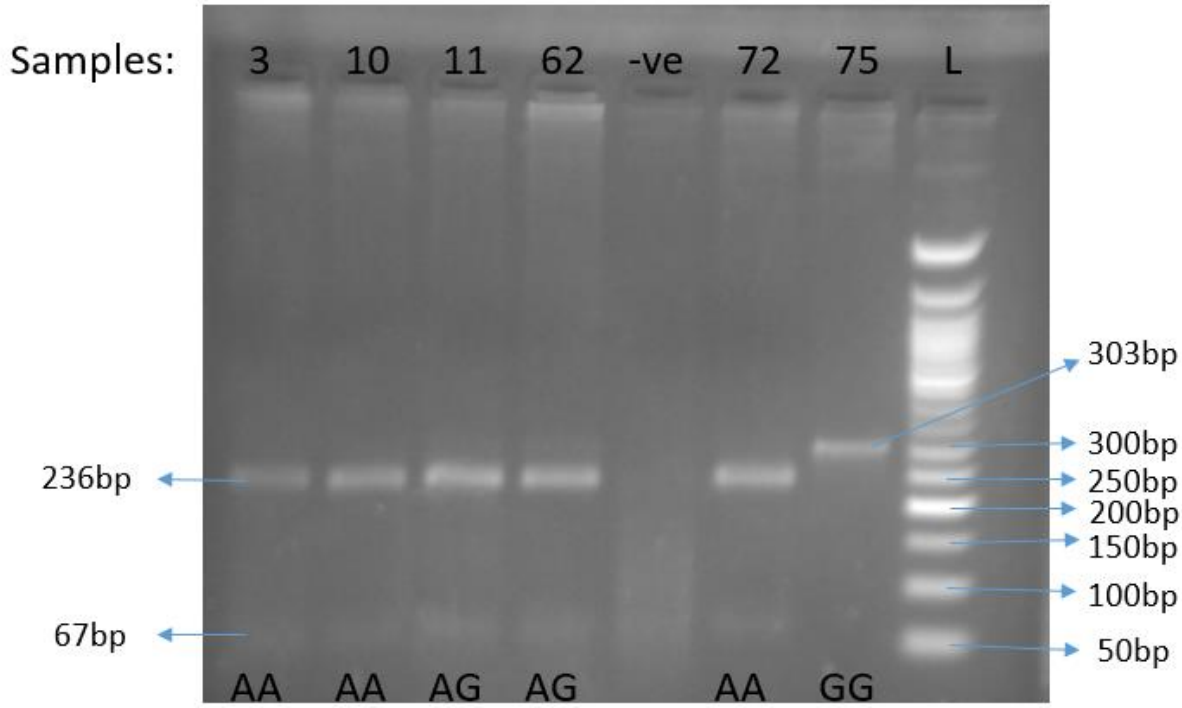

Fig 17 a) Agarose gel electrophoresis (3% agarose w/v) illustrating digestion of 6 DNA samples at single annealing temperatures 70˚C. (Expected band sizes and genotyes = GG: 303bp; AA: 236+67 bp; AG:303+236+67 bp.)

Lane1: DNA Sample 3; **Lane2**: DNA Sample 10; **Lane 3**: DNA Sample11; **Lane 4**: DNA sample 62; **Lane 5**: Negative control; **Lane 6**: DNA Sample72; **Lane 7**: DNA Sample 75; **Lane 8**: 50 bp Ladder.

b) rs61731956

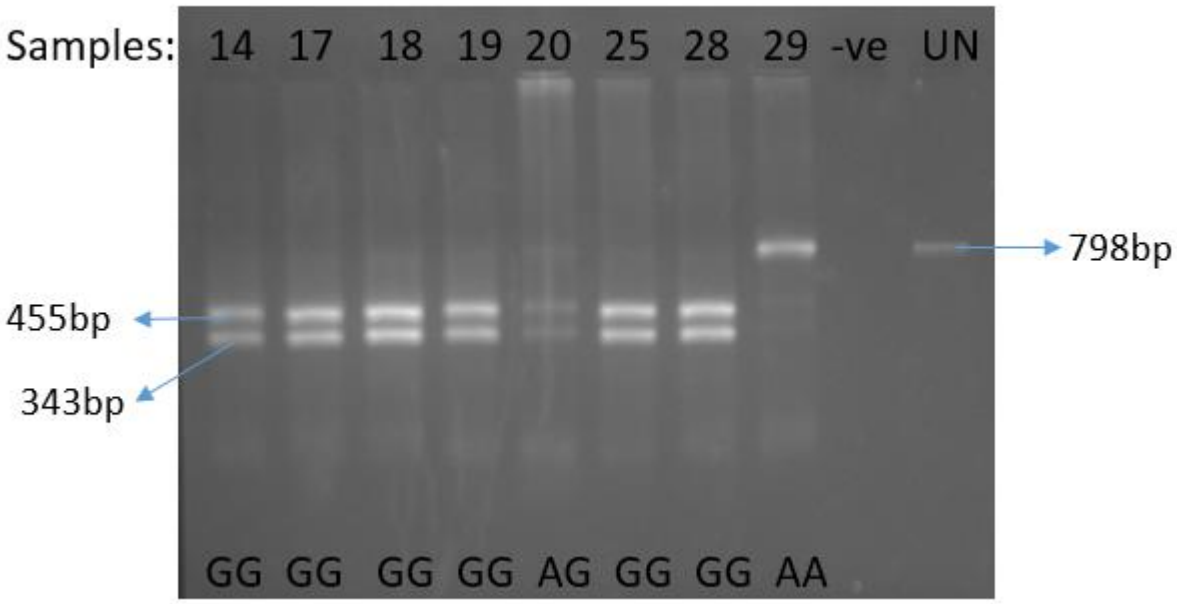

Fig 17 b) Agarose gel electrophoresis (1.5% agarose w/v) illustrating digestion of 6 DNA samples at single annealing temperatures 56˚C. (Expected band sizes and genotypes = AA: 798bp; GG: 455+343bp; AG:798+455+343 bp.)

Lane1: DNA Sample 14; **Lane2**: DNA Sample 17; **Lane 3**: DNA Sample18; **Lane 4**: DNA sample 19; **Lane 5**: DNA sample 20; **Lane 6**: DNA Sample 25; **Lane 7**: DNA Sample 28; **Lane 8**: DNA sample 29. **Lane 9**: Negative control; **Lane 10**: Undigested PCR product.

CHAPTER 6: DISCUSSION

Vitiligo is a chronic stigmatizing disease which mainly affects melanocytes from epidermis basal layer, leading to the development of white (depigmented) patches on the skin.

Upregulated expression of LXR-alpha in the melanocytes from perilesional skin as compared to normal skin of vitiligo patient speculates its role in vitiligo pathogenesis (Kumar, Parsad *et al*., 2010). In the present study, we investigated vitiligo patients for genetic variation in the LXR-alpha gene which may show association with vitiligo susceptibility. In our research, foremost step was to evaluate the nsSNPs computationally. Eventually, 6 nsSNPs of LXR-α gene were predicted to be significant by SIFT, which were then subjected to in-silico analysis by several tools like PROVEAN, PolyPhen, MutPred, SNPeffect, nsSNPAnalyzer, PANTHER, PhD-SNP, SuSPect, I-Mutant 2.0, and Tm-Align. Structural theoretical models of LXR- α were created using PSIPRED and Phyre2 server, which were further evaluated. Out of 6 nsSNPs, 3 nsSNPs (rs41275182, rs11545529 and rs61731956) were predicted to be damaging by SIFT and PROVEAN. Among the predicted, only one, rs61731956 was found to be highly deleterious by PhD-SNP, PANTHER and nsSNPAnalyzer. Additionally, I-Mutant and MuPro showed a decrease in stability for two nsSNPs (rs61731956 and rs78765998). Protein structural analysis was performed by using I-Mutant, Phyre2, MUSTER, Tm-Align and Discovery Studio softwares to check their molecular dynamics and energy minimization calculations. This study suggested that H339Q (rs78765998) and R355Q (rs61731956) variants of LXR-α gene have possible deleterious effects onto the protein activity. Such profiling of nsSNPs in LXR-α gene suggested that I39V (rs11545529), H339Q (rs78765998) and R355Q (rs61731956) variants of LXR-α gene have potential to introduce alterations in the protein stability and may influence the risk of vitiligo.

We further focused on investigating any association of nsSNPs, **rs11545529 (+10906 A >G) and rs61731956 (+19640 G >A)** in LXR-α with the risk of vitiligo in North Indian population. The two SNPs studied here were chosen on the basis of above-mentioned in-silico analysis of nsSNPs of LXR-alpha gene. Through the advantages of PCR-RFLP technique, genotypes were successfully obtained for the cases and control samples. Genotyping of the SNPs in the LXR-α gene revealed that the variant G allele of rs11545529 was found in 19% of controls and 21% of cases; the variant A allele of rs61731956 was found in 5% of controls and 7% of cases.

Consequently, appropriate statistical methods were applied to elucidate the association of variants with susceptibility of the disease.

The allelic frequencies of these two SNPs between vitiligo and control were, rs11545529: p=0.5197; rs61731956: p=0.5318, which suggested no association of minor allele of both the SNP with the vitiligo. As a result, **+10906** G and **+10906** A alleles were found to have no relation to the risk of vitiligo with respective statistical parameters as given below;

rs11545529: odds ratio (OR) =0.8462; 95% confidence interval (CI) =0.5090-1.4068; **rs61731956:** OR= 0.7568; 95% CI =0.31-1.81.

Therefore, the results showed that the selected variants were not significantly associated with the risk of vitiligo.

CHAPTER 7: CONCLUSION AND FUTURE PROSPECTS

Computational study has now got major importance to screen diseases specific SNP at molecular level. In this study in silico analysis has been performed to investigate the effect of nsSNPs on structure – function of LXR-alpha.

Sequence analysis results showed that mutations I39V (rs11545529) and R355Q (rs61731956) had lowest protein stability. Structural analysis results showed that the amino acid residue substitutions which had the greatest impact on the stability of the LXR-α protein were mutations H339Q (rs78765998) and R355Q (rs61731956).

Therefore, it has been concluded that two of these variants, rs11545529 and rs61731956 were found to be highly deleterious in their effects and could have the potential to increase the risk of vitiligo. This approach paved the way for researchers in prioritizing highly deleterious SNP's, and also in identifying and short listing ''candidate ns-SNPs'' for further confirmatory analysis.

Experimentally, the same results could not be established as the genotyping allelic frequencies of cases and control were not significant, which results in no association of the selected variants with vitiligo susceptibility. Although insignificant, this data could further be utilised in studying the etiological factors of this disease.

APPENDIX

1. GLASSWARES AND INSTRUMENTS

1.1 Glasswares

- Beaker – 1000 ml, 500ml, 100ml
- Capped Bottles
- Eppendorfs (autoclaved)- 2ml, 1.5ml, 0.5 ml and 0.2 ml
- PCR Tube stand
- Measuring cylinder – 500 ml, 100ml, 10 ml
- Eppendorfs stand
- Autoclaved Microtips (100-1000µl, 20-200µl, 0.1-10µl)

1.2 Instruments

- PCR Tube stand
- Rocker
- Micro pipette
- Spinner
- Thermo-Cycler
- Weighing balance
- Laminar Air Flow
- Refrigerator (-80º C, -20˚ C, 4˚C)
- Autoclave
- Nanodrop Spectrophotometer
- Incubator
- Vortex
- Hot air Oven
- Agarose Gel Electrophoresis chamber
- pH meter
- UV transilluminator
- MilliQ Water unit
- Centrifuge
- Microwave Oven
- Water Bath

2. REAGENTS

2.1) Di-sodium ethylene diamine tetra acetate, Na_2EDTA (0.5 M, pH 8.0)

• Take 186.1g of Na_2 EDTA and add to it 800ml of MilliQ Water.
• Stir Vigorously on Magnetic stirrer.
• Adjust pH to 8.0 with 10M NaOH.
• Make up the volume to 1000ml.

2.2) Tris (hydroxymethyl) aminomethane-chloride, Tris-Cl (1M, pH 8.0)

• Take 121.2g Tris Base in 800ml of distilled water.
• Adjust the pH to 8 by adding 1N HCl.
• Make up the volume to 1000ml with MQ water.
Solution was filtered through Whatmann filter paper and stored in a sterile tight screw capped reagent bottle

2.3) Tris –Cl (1 M; pH 7.3)

• Take 121.2g Tris Base in 800ml of distilled water
• Adjust the pH to 7.3 by adding 1N HCl.
• Make up the volume to 100ml with MQ water.
Solution was filtered through Whatmann filter paper and stored in a sterile tight screw capped reagent bottle

2.4) Ammonium Chloride, NH_4Cl (1 M)

• 53.5 g of ammonium chloride dissolved in 800ml MQ water.
• Make up the volume to 1000ml with MQ water.

2.5) 10% SDS

• Dissolve 10g SDS in 70ml of distilled water.
• Heat to 68^{o}C to mix the solution.
• Make up the volume to 100ml with MQ water.

2.6) Red Blood Cell Lysis Buffer

Composition: Tris 10mM, pH-8.0; EDTA 1mM; NH_4Cl 125 mM, pH 8.0

EDTA (0.5M) 2ml

Tris (1M , pH-8.0) 10ml

NH_4Cl (1M) 125 ml

Mixed the above reagent in MQ water to obtain the final volume of 1000 ml RBC lysis buffer.

2.7) Tris-EDTA (TE) buffer (pH 8.0)

Composition: Tris 10mM; EDTA 1mM, pH 8.0

EDTA (0.5M) 2ml

Tris (1M , pH-8.0) 10ml

Mixed the above reagent in MQ water to obtain the final volume of 1000 ml RBC lysis buffer.

2.8) Tris-EDTA (TE) buffer (pH 7.3)

Composition: Tris 10mM; EDTA 1mM, pH 7.3

EDTA (0.5 M) 2ml

Tris (1M, pH 7.3) 10ml

Mixed the above reagent in MQ water to obtain the final volume of 1000 ml RBC lysis buffer.

2.9) Ammonium Acetate (7.5 M)

- Dissolved 28.9g ammonium acetate salt in 20ml of MQ water
- The final volume was adjusted to 50 ml.

REFERENCES

1. Agarwal, S., Kaur, G., Randhawa, R., Mahajan, V., Bansal, R. & Changotra, H. (2016). Liver X Receptor-α polymorphisms (rs11039155 and rs2279238) are associated with susceptibility to vitiligo. Meta Gene, 8, 33–36.
2. al Badri, A.M., Foulis, A.K., Todd, P.M., Gariouch, J.J., Gudgeon, J.E., Stewart, D.G., Gracie, J.A. & Goudie, R.B. (1993). Abnormal expression of MHC class II and ICAM-1 by melanocytes in vitiligo. J Pathol. Feb;169(2):203-6.
3. Ala, Y., Pasha, M. K., Rao, R. N., Komaravalli, P. L. & Jahan, P. (2015). Association of IFN-γ: IL-10 Cytokine Ratio with Nonsegmental Vitiligo Pathogenesis. Autoimmune Diseases, 423490.
4. Allam, M. & Riad H. (2013) Concise review of recent studies in vitiligo. Qatar Med J. 1–19.
5. Alikhan, A., Felsten, L.M., Daly, M. & Petronic-Rosic, V. (2011) Vitiligo: a comprehensive overview Part I. Introduction, epidemiology, quality of life, diagnosis, differential diagnosis, associations, histopathology, etiology, and work-up. J Am Acad Dermatol. Sep;65(3):473-91.
6. Anbar Tel, D., Abdel-Raouf, H., et al. (2011). Perifollicular inflammatory infiltrate in vitiligo. Int J Dermatol 50(2): 234-237.
7. Beazley, W.D., Gaze, D., Panske, A., et al. (1999). Serum selenium levels and blood glutathione peroxidase activities in vitiligo. Br J Dermatol 141:301–3.
8. Bensinger, S. J. and Tontonoz, P. (2008). Integration of metabolism and inflammation by lipid-activated nuclear receptors. Nature 454(7203): 470-477.
9. Billoni, N., Buan, B., et al. (2000). Expression of peroxisome proliferator activated receptors (PPARs) in human hair follicles and PPAR alpha involvement in hair growth. Acta Derm Venereol 80(5): 329-334.
10. Bhagwat, M. (2010). Searching NCBI's dbSNP database. Curr. Protoc. Bioinformatics. (Chapter 1: Unit 1.19).
11. Bindoli, A., Rigobello, M. P., et al. (1992). Biochemical and toxicological properties of the oxidation products of catecholamines. Free Radic Biol Med 13(4): 391-405.

12. Buchan, D.W.A., Minneci, F., Nugent, T.C.O., Bryson, K. & Jones, D.T. (2013). Scalable web services for the PSIPRED Protein Analysis Workbench. Nucleic Acids Res. 41, W340–W348.
13. Casp, C.B., She, J.X. & McCormack, W.T. (2002). Genetic association of the catalase gene (CAT) with vitiligo susceptibility. Pigment Cell Res. Feb;15(1):62-6.
14. Chen, Y. S., Li, F. J., et al. (2008). Study on the probability of hepatitis B virus infection at public service places. Zhonghua Liu Xing Bing Xue Za Zhi 29(7): 689-692.
15. Choi, Y., Sims, G.E., Murphy, S., Miller, J.R., & Chan, A.P., (2012). Predicting the functional effect of amino acid substitutions and indels. PLoS One 7, e46688.
16. Chu, D.H. (2008). Overview of biology, development, and structure of skin. In K. Wolff, L.A. Goldsmith, S.I. Katz, B.A. Gilchrest, A.S. Paller, & D.J. Leffell (Eds.), Fitzpatrick's dermatology in general medicine (7th ed., pp. 57–73). New York: McGraw-Hill.
17. Colucci, R., Lotti, F., Dragoni, F., Arunachalam, M., Lotti, T., Benvenga, S. & Moretti, S. (2014). High prevalence of circulating autoantibodies against thyroid hormones in vitiligo and correlation with clinical and historical parameters of patients. Br J Dermatol.171(4):786-98.
18. Colucci, R., Dragoni, F. & Moretti, S. (2015). Oxidative Stress and Immune System in Vitiligo and Thyroid Diseases. Oxidative Medicine and Cellular Longevity, 631927.
19. Costin, G.E. & Hearing, V.J. (2007). Human skin pigmentation: melanocytes modulate skin color in response to stress. FASEB J. 21(4):976-94.
20. Cui, R., Widlund, H. R., et al. (2007). Central role of p53 in the suntan response and pathologic hyperpigmentation. Cell 128(5): 853-864.
21. Denat, L., Kadekaro, A. L., et al. (2014). Melanocytes as instigators and victims of oxidative stress. J Invest Dermatol 134(6): 1512-1518.
22. Dinarello, C.A. (2011). Interleukin-1 in the pathogenesis and treatment of inflammatory diseases. Blood. 117(14):3720–3732.
23. Dupin, E., Real, C., Glavieux-Pardanaud, C., Vaigot, P. and Le Douarin, N.M. (2003). Proc. Natl. Acad. Sci. USA, Apr. 17.

24. Dwivedi, M., Laddha, N. C., Shah, K., Shah, B. J., & Begum, R. (2013). Involvement of Interferon-Gamma Genetic Variants and Intercellular Adhesion Molecule-1 in Onset and Progression of Generalized Vitiligo. Journal of Interferon & Cytokine Research, 33(11), 646–659.
25. Faria, A.R., et al. (2014). Vitiligo - Part 2 - classification, histopathology and treatment. An. Bras. Dermatol. vol.89, n.5 pp.784-790.
26. Garcia-Melendez, M.E., Salinas-Santander, M., Sanchez-Dominguez, C., et al. (2014). Protein tyrosine phosphatase PTPN22 +1858C/T polymorphism is associated with active vitiligo. Experimental and Therapeutic Medicine. 8(5):1433-1437.
27. Gauthier, Y., Cario Andre, M. & Taïeb, A. (2003). A critical appraisal of vitiligo etiologic theories. Is melanocyte loss a melanocytorrhagy?. Pigment Cell Res. Aug;16(4):322-32.
28. Glassman, S.J. (2011). Vitiligo, reactive oxygen species and T-cells. Clin Sci (Lond). Feb;120(3):99-120.
29. Haake, A.R. & Hollbrook, K. (1999). The structure and development of skin. In I. Freedberg, A. Eisen, K. Wolff, K. Austen, L. Goldsmith, S. Katz, et al. (Eds.), Fitzpatrick's dermatology in general medicine (5th ed., pp. 70–111). New York: McGrawHill.
30. Hara, M., Yaar, M., Tang, A., Eller, M.S., Reenstra, W. & Gilchrest, B.A. (1994). Role of integrins in melanocyte attachment and dendricity. J Cell Sci. Oct;107 (Pt 10):2739-48.
31. Huang, Y., Yi, X., Jian, Z., Wei, C., Li, S., Cai, C., Zhang, P., Li, K., Guo, S., Liu, L., Shi, Q., Gao, T. & Li, C. (2013). A single-nucleotide polymorphism of miR-196a-2 and vitiligo: an association study and functional analysis in a Han Chinese population. Pigment Cell Melanoma Res. 26(3):338-47.
32. Jamal, S. & Schneider, R.J. (2002). UV-induction of keratinocyte endothelin-1 downregulates E-cadherin in melanocytes and melanoma cells. J Clin Invest. 110:443-52.
33. James, W.D., Berger, T.G. & Elston, D.M. (2006). Andrews' diseases of the skin: Clinical dermatology (10th ed.). Philadelphia: Elsevier Saunders.

34. Jamroz-Wisniewska, A., Wojcicka, G., et al. (2007). Liver X receptors (LXRs). Part II: non-lipid effects, role in pathology, and therapeutic implications. Postepy Hig Med Dosw (Online) 61: 760-785.
35. Kanitakis, J. (2002) Anatomy, histology and immunohistochemistry of normal human skin. Eur J Dermatol. Jul-Aug;12(4):390-9.
36. Kelley, L.A. & Sternberg, M.J.E. (2009). Protein structure prediction on the web: a case study using the Phyre server. Nat. Protoc. 4, 363–371.
37. Klarquist, J. et al (2010). Reduced skin homing by functional Treg in vitiligo. Pigment Cell Melanoma Res, 23(2):276-86.
38. Kluger, N., Cotten, H., et al. (2008). Dermatofibroma occurring within a tattoo: report of two cases. J Cutan Pathol 35(7): 696-698.
39. Kohro, T., Nakajima, T., Wada, Y., et al. (2000) Genomic structure and mapping of human orphan receptor LXR alpha: upregulation of LXR-α mRNA during monocyte to macrophage differentiation. J Atheroscler Thromb. 7(3):145-51.
40. Komuves, L. G., Schmuth, M., et al. (2002). Oxysterol stimulation of epidermal differentiation is mediated by liver X receptor-beta in murine epidermis. J Invest Dermatol 118(1): 25-34.
41. Kotobuki, Y., Tanemura, A., Yang, L., Itoi, S., Wataya-Kaneda, M., Murota, H., Fujimoto, M., Serada, S., Naka, T. & Katayama, I. (2012). Dysregulation of melanocyte function by Th17-related cytokines: significance of Th17 cell infiltration in autoimmune vitiligo vulgaris. Pigment Cell Melanoma Res, 25(2):219-30.
42. Kruger, C. & Schallreuter, K.U. (2015). Stigmatisation, Avoidance Behaviour and Difficulties in Coping are common Among Adult Patients with Vitiligo. Acta Derm Venereol, 95(5):553-8.
43. Kumar, R. & Parsad, D., et al. (2010). Liver X receptor expression in human melanocytes, does it have a role in the pathogenesis of vitiligo?. Exp Dermatol 19(1): 62-64.
44. Kumar, R., Parsad, D. & Kanwar, A.J. (2011). Role of apoptosis and melanocytorrhagy: A comparative study of melanocytes adhesion in stable and unstable vitiligo. Br J Dermatol 164:187-91

45. Kumar, R., Parsad, D., Kanwar, A.J. & Kaul, D. (2012). Altered levels of LXR-α: crucial implications in the pathogenesis of vitiligo. Exp Dermatol. 21(11):853-8.
46. Kummer, J.A, et al. (2007). Inflammasome components NALP 1 and 3 show distinct but separate expression profiles in human tissues suggesting a site-specific role in the inflammatory response. J Histochem Cytochem. 55(5):443–452.
47. Laddha, N.C., Dwivedi, M. & Begum, R. (2012). Increased Tumor Necrosis Factor (TNF)-α and Its Promoter Polymorphisms Correlate with Disease Progression and Higher Susceptibility towards Vitiligo. PLoS One. 7(12): e52298.
48. Le Poole, I.C., Das, P.K., van den Wijngaard, R.M., Bos, J.D. & Westerhof, W. (1993). Review of the etiopathomechanism of vitiligo: a convergence theory. Exp Dermatol. Aug;2(4):145-53.
49. Le Poole, I.C., van den Wijngaard, R.M., Westerhof ,W. & Das, P.K. (1997). Tenascin is overexpressed in vitiligo lesional skin and inhibits melanocyte adhesion. Br J Dermatol. Aug;137(2):171-8.
50. Lee, C. S. & Park, M. et al. (2013). Liver X receptor activation inhibits melanogenesis through the acceleration of ERK-mediated MITF degradation. J Invest Dermatol 133(4): 1063-1071.
51. Lei, T. C., Vieira, W. D., et al. (2002). In vitro migration of melanoblasts requires matrix metalloproteinase-2: implications to vitiligo therapy by photochemotherapy. Pigment Cell Res 15(6): 426-432
52. Lerner, A. B. (1959). Vitiligo. J Invest Dermatol 32(2, Part 2): 285-310.
53. Levy, C., Khaled, M., et al. (2006). MITF: master regulator of melanocyte development and melanoma oncogene. Trends Mol Med 12(9): 406-414.
54. Li, B., (2009). Automated inference of molecular mechanisms of disease from amino acid substitutions. Bioinformatics 25, 2744–2750.
55. Lin, J.Y. & Fisher, D.E. (2007). Melanocyte biology and skin pigmentation. Nature. Feb 22;445(7130):843-50.
56. Lu, L., Liu, L., Ji, Y., Jin, H. & He, L. (2014). Association of the 389 C/T polymorphism of the catalase gene with susceptibility to vitiligo: a meta-analysis. Clin Exp Dermatol. 39(4):454-60.

57. Luu, T.D., Rusu, A.M., Walter, V., Ripp, R. & Moulinier, M.S.V (2012). 3d: database of human MisSense Variants mapped to 3D protein structure. Database (Oxford);3
58. Majumder, P.P., Nordlund, J.J. & Nath, S.K. (1993). Pattern of familial aggregation of vitiligo. Arch Dermatol. 129:994–998.
59. Marín-Martín, F.R., Soler-Rivas, C., Martín-Hernández, R. & Rodriguez-Casado, A. (2014). A Comprehensive In- Silico Analysis of the Functional and Structural Impact of Nonsynonymous SNPs in the ABCA1 Transporter Gene. Cholesterol Volume. Article ID 639751, 19 pages.
60. Mayor, R. & Theveneau, E. (2013). The neural crest. Development. Jun;140(11):2247-51.
61. Martinon, F., Gaide, O., Pétrilli, V., Mayor, A. & Tschopp, J. (2007). NALP inflammasomes: A central role in innate immunity. Semin Immunopathol. 29(3):213–229.
62. McGill, G. G., et al (2002). Bcl2 Regulation by the Melanocyte Master Regulator Mitf Modulates Lineage Survival and Melanoma Cell Viability. Cell volume 109 issue 6 p707–718.
63. Mehaney, D.A., Darwish, H.A., Hegazy, R.A., et al. (2014). Analysis of Oxidative Stress Status, Catalase and Catechol-O-Methyltransferase Polymorphisms in Egyptian Vitiligo Patients. PLoS One. 9(6): e99286.
64. Miller, S. A., Dykes, D. D., & Polesky, H. F. (1988). A simple salting out procedure for extracting DNA from human nucleated cells. Nucleic Acids Research, 16(3), 1215.
65. Mohammed, G. F., Gomaa, A. H. et al. (2015). Highlights in pathogenesis of vitiligo. World J Clin Cases 3(3): 221-230.
66. Mort, R.L., Jackson, I.J. & Patton, E.E. (2015). The melanocyte lineage in development and disease. Development. 142: 620-632.
67. Mu, E.W., Cohen, B.E. & Orlow, S.J. (2015). Early-onset childhood vitiligo is associated with a more extensive and progressive course. J Am Acad Dermatol. Sep;73(3):467-70.
68. Ng, P.C., & Henikoff, S. (2003). SIFT: predicting amino acid changes that affect protein function. Nucleic Acids Res. 31 (13), 3812–3814.

69. Panja, S. K., Bhattacharya, B., et al. (2013). Role of histamine as a toxic mediator in the pathogenesis of vitiligo. Indian J Dermatol 58(6): 421-428.
70. Park, H. Y., Kosmadaki, M., et al. (2009). Cellular mechanisms regulating human melanogenesis. Cell Mol Life Sci 66(9): 1493-1506.
71. Rodriguez-Casado, A. (2012). In silico investigation of functional nsSNPs – an approach to rational drug design. Dovepress Volume 2012:2 Pages 31—42.
72. Russell, L. E., Harrison, W. J., et al. (2007). Characterization of liver X receptor expression and function in human skin and the pilosebaceous unit. Exp Dermatol 16(10): 844-852.
73. Schallreuter, K. U., Bahadoran, P., Picardo, M., et al. (2008). Vitiligo pathogenesis: autoimmune disease, genetic defect, excessive reactive oxygen species, calcium imbalance, or what else?. Experimental Dermatology, vol. 17, no. 2, pp. 139–140.
74. Schallreuter, K. U., Wood, J. M., et al. (1996). Increased monoamine oxidase A activity in the epidermis of patients with vitiligo. Arch Dermatol Res 288(1): 14-18.
75. Schallreuter, K. U., Wood J. M., et al. (1994). Regulation of melanin biosynthesis in the human epidermis by tetrahydrobiopterin. Science 263(5152): 1444-1446.
76. Schallreuter, K.U., Moore, J, Wood, J.M., et al (1999). In vivo and in vitro evidence for hydrogen peroxide (H_2O_2) accumulation in the epidermis of patients with vitiligo and its successful removal by a UVB-activated pseudocatalase. J Investig Dermatol Symp Proc. Sep;4(1):91-6.
77. Schallreuter, K.U., Wood, J.M. & Berger, J. (1991). Low catalase levels in the epidermis of patients with vitiligo. J Invest Dermatol. Dec;97(6):1081-5.
78. Shajil, E. M., Chatterjee, S., et al. (2006). Vitiligo: pathomechanisms and genetic polymorphism of susceptible genes. Indian J Exp Biol 44(7): 526-539.
79. Simon, J. D., Peles, D., et al. (2009). Current challenges in understanding melanogenesis: bridging chemistry, biological control, morphology, and function. Pigment Cell Melanoma Res 22(5): 563-579.
80. Slominski, A., Tobin, D.J., Shibahara, S. & Wortsman, J. (2004) Melanin pigmentation in mammalian skin and its hormonal regulation. Physiol Rev. Oct;84(4):1155-228.

81. Spritz, R.A. (2006). The genetics of generalized vitiligo and associated autoimmune diseases. J Dermatol Sci. 41:3–10
82. Spritz, R.A. (2013). Modern vitiligo genetics sheds new light on an ancient disease. J Dermatol. May;40(5):310-8. doi: 10.1111/1346-8138.12147.
83. Spritz, R.A. (2010). The genetics of generalized vitiligo: autoimmune pathways and an inverse relationship with malignant melanoma. Genome Med. 2(10):78
84. Steffensen, K. R. and Gustafsson, J. A. (2004). Putative metabolic effects of the liver X receptor (LXR). Diabetes 53 Suppl 1: S36-42.
85. Swalwell, H., Latimer, J., et al. (2012). Investigating the role of melanin in UVA/UVB- and hydrogen peroxide-induced cellular and mitochondrial ROS production and mitochondrial DNA damage in human melanoma cells. Free Radic Biol Med 52(3): 626-634.
86. Syvänen, A.C. (2001). Accessing genetic variation: genotyping single nucleotide polymorphisms. Nat Rev Genet. Dec;2(12):930-42.
87. Taieb, A. (2000). Intrinsic and extrinsic pathomechanisms in vitiligo. Pigment Cell Res 13 Suppl 8: 41-47.
88. van den Wijngaard, R.M., Aten, J., Scheepmaker, A., Le Poole, I.C., Tigges, A.J., Westerhof. W. & Das, P.K. (2000). Expression and modulation of apoptosis regulatory molecules in human melanocytes: significance in vitiligo. Br J Dermatol. Sep;143(3):573-81.
89. Videira, I. F., Moura, D. F., et al. (2013). Mechanisms regulating melanogenesis. An Bras Dermatol 88(1): 76-83.
90. Wang, D.G., et al. (2008). Large-Scale Identification, Mapping, and Genotyping of Single-Nucleotide Polymorphisms in the Human Genome. Science. Vol. 280, Issue 5366, pp. 1077-1082.
91. Whiton, M. E., Pinart, M., Batchelor, J., et al. (2015). Interventions for vitiligo. Cochrane Database of Systematic Reviews, no. 1, Article ID CD003263.
92. Willy, P. J., Umesono, K., et al. (1995). LXR, a nuclear receptor that defines a distinct retinoid response pathway. Genes Dev 9(9): 1033-1045.
93. Wu, S. & Zhang, Y. (2008). MUSTER: improving protein sequence profile–profile alignments by using multiple sources of structure information. Proteins 72, 547–556.

94. Yates, C.M. & Sternberg, M.J. (2013). The effects of non-synonymous single nucleotide polymorphisms (nsSNPs) on protein-protein interactions. J Mol Biol. Nov 1;425(21):3949-63.